Arabian Journal of Chemistry (2020) **13**, 7773–7797

King Saud University

Arabian Journal of Chemistry

www.ksu.edu.sa
www.sciencedirect.com

ORIGINAL ARTICLE

Antitumor effect of guava leaves on lung cancer: A network pharmacology study

Lirong Jiang [a,b], Junyu Lu [a,b], Yue Qin [a,b,*], Weirong Jiang [a], Yanping Wang [a,b]

[a] *College of Chemistry and Bioengineering, Hechi University, Hechi 546300, China*
[b] *Guangxi Key Laboratory of Microbiology and Plant Resources Development, Hechi University, Hechi 546300, China*

Received 10 June 2020; accepted 6 September 2020
Available online 21 September 2020

KEYWORDS

Guava leaf;
Antitumor;
Network pharmacology;
SystemsDock molecular docking

Abstract Guava is known for its hypoglycemic, antivirus, antibacterial, anti-inflammatory, antioxidant, and antitumor properties. In this study, triterpenoids, sesquiterpenes, and flavonoids were examined as potential targets of constituents of guava leaves. Our study was aimed to reveal the antitumor mechanism and construct the network pharmacology network of guava leaf constituents and lung cancer. The potential targets of guava leaf constituents were searched in target databases, while the disease genes were searched in the GeneCards database. The common targets of drugs and diseases were screened out. A network map was constructed by the Cytoscape software, and the GO and KEGG pathways were analyzed. The existing cases were studied by SystemsDock molecular docking and cBioPortal tumor database study. Among the 66 chemical constituents of guava leaves, 153 of their targets were the lung cancer genes involved in many signaling pathways, such as the PI3K-Akt signaling pathway, in small cell lung cancer and non-small cell lung cancer. There was a binding activity between ligand compounds and receptor proteins. Guava leaves inhibited tumor through a gene regulatory network, and may play an important role in gene-targeting therapy. Through network pharmacology, we found that guava leaves had potential targets that interacted with various tumors, regulating the signaling pathways of cancers. This study preliminarily verified the pharmacological basis and the mechanism of the antitumor effect of guava leaves, providing a foundation for further research.

1. Introduction

Guava (*Psidium guajava*), a member of the *Myrtaceae* family, is an evergreen shrub or small arbor with a wide range of habitats. Guava is found in countries in tropical or subtropical areas such as South America, Africa, and Southern Asia (Gutierrez et al., 2008; Feng et al., 2015). Guava leaves, also known as *Folium Psidii Guajavae*, are the dry leaves and leafy shoots of guava. The substances in guava leaves are triter-

* Corresponding author at: Hechi University, No. 42 Longjiang Road, Hechi 546300, China.
E-mail address: qinyuehechi@outlook.com (Y. Qin).
Peer review under responsibility of King Saud University.

Production and hosting by Elsevier

https://doi.org/10.1016/j.arabjc.2020.09.010
1878-5352

penoids (Shao et al., 2012a), flavonoids, tannins (Seo et al., 2014), sesquiterpenes, miscellaneous quinones, volatile oils, and benzophenone glycosides. Guava is known for its hypoglycemic, antivirus, antibacterial, anti-inflammatory, antioxidant, and antitumor properties (Seo et al., 2014). These substances in guava leaves are of great research value. In a previous study, researchers identified novel types of aldehyde terpenes with their spectral characteristics and summarized the chemical structures of 17 heterodialdehyde compounds (Ouyang et al., 2015). Moreover, Psiguadial C and Psiguadial D showed significant biological activities, including the inhibitions of protein tyrosine phosphatase 1B (PTP1B) and human hepatoma cells (HepG2) (Shao et al., 2012b). Triterpenoids are known to exert antitumor effects (Song and Zhu, 2011; Lu et al., 2016). Flavonoids are one of the main functional components in guava leaves and have various pharmacological effects (Alnaqeeb et al., 2019; Luo et al., 2019). Researchers extracted flavonoids from guava leaves and obtained approximately 9.89 mg/g of total flavonoids (Wang et al., 2016b). Flavonoids in plants are also known for their antitumor activity, which mainly involves regulation of immune function, repression of tumor cell adhesion and signal transmission, and inhibition of cellular proliferation and tumor angiogenesis (Kandaswami et al., 2005). In this study, triterpenoids, sesquiterpenes, and flavonoids were examined as potential targets of guava leaves.

Previous studies have investigated antitumor substances in guava leaves. It was found that guava leaf extracts exhibit potent antitumor activity (Ashraf et al., 2016)and play an inhibitory role in HeLa and Ec109 cells (Lee and Park, 2010).

Lung cancer has been the leading cause of cancer deaths among men since the early 1950s. A total of 1,824,701 lung cancer cases were estimated worldwide in 2012, accounting for nearly 32% for women and 68% for men (Rafiemanesh et al., 2016). In contrast, a total of 1,589,925 lung cancer deaths were estimated in 2012, of which 31% were women and 69% were men (Rafiemanesh et al., 2016). The number of new lung cancer cases has risen to 7,328,000, and 5,807,000 deaths occurred in China in 2013 (Chen et al., 2017). Lung cancer is the most common malignant tumor in China with high morbidity and mortality rates (Xing et al., 2019). Therefore, finding ways to treat lung cancer is of vital importance.

The concept of network pharmacology is based on multidisciplinary theories such as systems biology and multidirectional pharmacology (Boezio et al., 2017). Utilizing various techniques, such as omics, high-throughput screening, network visualization, and network analysis can help us better understand the molecular mechanism of diseases and the pharmacological mechanism of drugs from a multidimensional perspective (Wu and Wu, 2015; Danhof, 2016; Boezio et al., 2017). The method of network pharmacology and the databases available for research also tend to be diverse (Hu et al., 2014; Lee, 2015; Wang et al., 2019). It is straightforward in visual analysis of the results through target prediction, pharmacological mechanism research, active component research, and construction of network graphs (Boezio et al., 2017).

Herein, we aimed to construct the network pharmacology of constituents from guava leaves and investigate the potential of these constituents on lung cancer.

2. Materials and methods

2.1. Materials

The databases used in this study included TCMSP, PubChem, PharmMapper, STRING, UniProt, GeneCards, Venny 2.1.0, KOBAS 3.0, SystemsDock, DisGeNET, and CbioPortal. The software used included ChemDraw Office 2010 (PerkinElmer), Cytoscape 3.7.1 (Cytoscape), and FunRich 3.1. 3 (http://www.funrich.org/download).

2.2. Methods

2.2.1. Collection of active constituents and chemical structures

Ouyang et al. (2015) systematically sorted out the compounds found in guava leaves through literature research; thus, these two documents were used as standards. The 2D or 3D structure of the target compound was searched in the PubChem (Kim et al., 2016) database, but for some of the compounds that were not included in the database, the chemical structure was drawn using the ChemBioDraw Ultra 12.0 software (PerkinElmer).

2.2.2. Screening of potential targets and acquisition of disease genes

Screening of potential targets: the TCMSP (Ru et al., 2014) database was used for the screening of potential targets, using "Chemical name" as the key word and the English name of the target compound as the potential target. PharmMapper (Liu et al., 2010) was used to screen potential targets. The 2D or 3D structures of the compound were used as input to screen potential targets. All potential targets of guava leave constituents were converted to gene names using the STRING database and the UniProt database, and the species selected was *Homo Sapiens*.

2.2.3. Acquisition of disease genes

Through the human gene database GeneCards, using "Lung cancer" as a key word, disease target genes with greater correlation with lung cancer were extracted, and the first 500 genes (based on the descending order of the correlation score) were selected as disease genes.

The searched potential target genes were compared with the disease genes in the Venny database, and the common genes were selected to obtain potential targets for the treatment of lung cancer with guava leaf constituents.

2.2.4. Topological analysis of target protein networks and gene assignment

The STRING database was used for gene regulatory network construction based on potential targets of guava leaf constituents and lung cancer genes. The species was set to "*Homo sapiens*" and the minimum interaction threshold was set to 0.97. PPI network interaction maps of potential targets of guava leaf constituents derived from the database was downloaded. Network topology analysis was performed using the Cytoscape (Kohl et al., 2011) database. The gene type was assigned to the gene through the DisGeNET (Bauer-Mehren et al., 2010) database, and the protein/gene was sequentially input for retrieval of the related gene and the target type

(protein class) information. Interactions between compounds and target proteins were analyzed by constructing a network map of "Guava leaf - constituent category - active constituent - gene".

2.2.5. GO and KEGG enrichment analysis

GO analysis was performed using the ClueGO plug-in in the Cytoscape software, and the gene symbols of targets of guava leaf constituent for lung cancer were input into ClueGO for gene ontology (GO) enrichment analysis (Biology Process, Molecular Function and Cellular Component). The gene symbols of targets of guava leaf constituent for lung cancer were converted into Entrez ID by the Funrich software, and KEGG pathway enrichment analysis was performed using KOBAS 3.0.

2.2.6. Molecular docking

The 10 genes that were relatively strong in the network diagram of "Guava leaf - constituent category - active constituent - gene" were molecularly docked with five compounds by systemsDock (Hsin et al., 2013; Hsin et al., 2016).

2.2.7. cBioportal analysis

The gene expression of existing case samples in the database was analyzed by cBioportal. cBioportal was financially funded by the Memorial Sloan-Kettering Cancer Center. It mainly addresses a large number of data problems obtained from large sample tumor genomic studies so that the results can be easily explored and directly applied to oncology (Wu et al., 2019).

2.2.8. Gene expression analysis and pathway activity analysis

The mRNA expression and the pathway activity of genes of interest were analyzed in the GSCALite database (http://bioinfo.life.hust.edu.cn/web/GSCALite/) following the instructions provided in this platform.

3. Results

3.1. Collection of active ingredients and their chemical structures

The 2D or 3D structures of all compounds were searched in the PubChem database, and the files in the sdf format were saved. Compounds not included in the database were identified by chemical structure, which were then drawn using the ChemDraw Ultra 12.0 software, and the sdf file was saved (Fig. 1). The structures of the compounds were searched by PubChem, and their molecular formulas and accession numbers in the database (PubChem CID) were retrieved. The relevant information of the active constituents of Guava leaves is listed in Table 1. In total, 66 active components of guava leaves, including 17 triterpenoids such as ursane and oleanane pentacyclic triterpenes, 19 sesquiterpenoids, and 30 flavonoids.

3.2. Screening of potential targets and acquisition of disease genes

A total of 115 potential targets for four triterpenoids and 303 potential targets for the 19 flavonoids were obtained from the TCMSP database (Table 2). Molecular information on guava leaves, including Lipinski's "five-law" parameters, namely relative molecular mass (MV), octanol–water partition coefficient (AlogP), possible hydrogen bond donor number (Hdon), possible hydrogen, number of bond receptors (Hacc), number of bonds allowed to rotate freely (RBN), oral bioavailability (OB), and drug-like degree (DL) were obtained. The targets of the active ingredients of guava leaves were obtained from the PharmMapper database, and targets with z'-score ≥ 1 were screened as potential targets of guava leaf active ingredients. From the definition in the database website, "Fit Score" and "z'-score" are scores generated by the metric's Fit score, which is a pre-calculated library score matrix, and a large positive z'-score represents the target-to-query combination. A total of 198 target genes for triterpenoids, 215 target genes for sesquiterpenoids, and 302 target genes for flavonoids were retrieved from the PharmMapper database. A total of 246 potential targets for triterpenoids, 215 potential targets for sesquiterpenoids, and 535 potential targets for flavonoids were obtained from TCMSP and Pharmmapper. The names of all potential targets were imported into the STRING database and Uniprot database, and converted into Gene Symbols.

In the Genecards database, with "Lung Cancer" as the key word, a total of 20,649 results were associated with lung cancer, and the top 500 targets with "Score" values ranged in descending order.

The genes associated with the three types of compounds were compared with the lung cancer genes in the Venny 2.1.0 database, and a chart of gene interaction was obtained (Fig. 2A). A total of 153 genes were obtained from lung cancer, and the target genes of guava leaf constituents against lung cancer were obtained. The total number of genes was 16.4%. Among them, there were 4 (0.4%) cross-reactive genes in three sputum and lung cancer; 68 (7.3%) cross-genes between flavonoids and lung cancer; 3 (0.3%) genes between triterpenoids, sesquiterpenes, and lung cancer; 9 (1%) cross-linking genes for scorpion, flavonoids, and lung cancer; 27 (2.9%) cross-linking genes for triterpenoids, flavonoids, and lung cancer; and 42 (4.5%) cross-linking genes for triterpenoids, sesquiterpenes, flavonoids, and lung cancer.

3.3. Topological analysis of target protein networks and gene assignment

The 153 targets related to lung cancer and identified as targets for guava leaf constituents were introduced into the STRING database to obtain a protein interaction network. Topological analysis of the target protein network was performed in Cytoscape. The topological analysis results are shown in Fig. 2B. The color depth and size of the nodes represent the strength of interaction between the gene and other genes. The interaction network had a total of 153 number of nodes. The number of edges associated with the target protein was 443, and the average node degree was 5.79, with p value (PPI enrichment p-value) $< 1.0e{-}16$. The target genes with a degree greater than or equal to 10 in the guava leaf constituent and lung cancer cross-linking network topology analysis were sequentially introduced into the DisGeNET database to obtain the protein type corresponding to the target. The results showed that the types of these proteins were nucleic acid binding, transcription factor, calcium-binding protein, kinase, transferase, signaling molecule, enzyme modulator, receptor, hydrolase, protease,

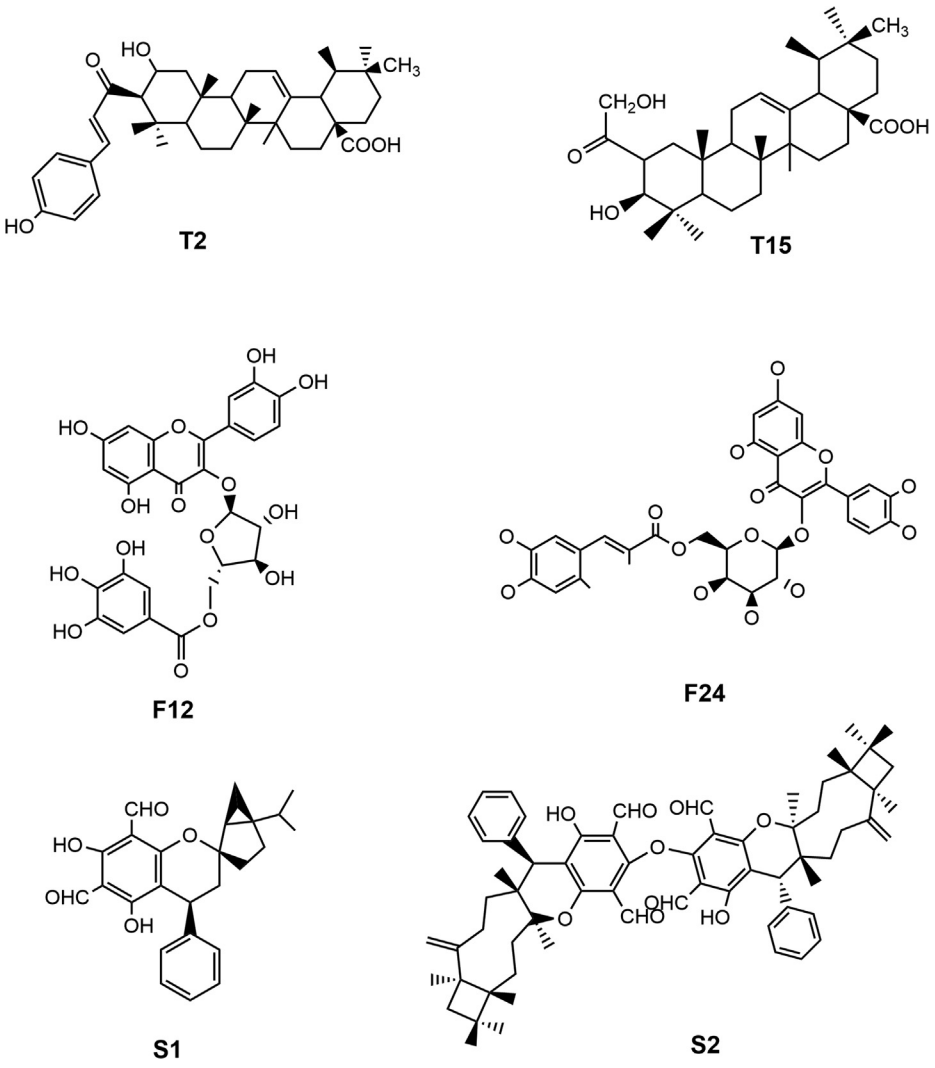

Fig. 1 The structural formula of six compounds, which were found but not included in the PubChem database. T2: 3β-O-trans-p-coumaroylmaslinicacid; T15: psidiumoic acid; F12: guavinoside C; F24: quercetin-3-O-(6″-feruloyl); S1: Diguajadial; S2: Guadial A.

and transfer/carrier protein (Table 3). The network topological analysis of genes associated with lung cancer in guava leaves genes with a score of 10 or higher and their genes are also shown in Table 3.

3.4. Cytoscape network interaction analysis

There is a genetic interaction between drugs and diseases. This is a characteristic of multi-component and multi-target network pharmacology analysis. Through Cytoscape network visualization analysis, a "Guava leaf-compound class-active ingredient-gene" interaction network was obtained. The compound and target information on nodes ≥20 are listed in Table 4, where the Average Shortest Path Length is the average shortest path, Closeness Centrality is the center proximity, and Radiality is the radial degree.

As shown in Fig. 3 and Table 4, the three compounds in guava leaves that interacted strongly with lung cancer were quercetin, genistein, and apigenin. Moreover, the top ten targets were vitamin D3 receptor (VDR), cyclin-dependent kinase 2 (CDK2), dual specificity mitogen-activated protein kinase 1 (MAP2K1), cyclin-dependent kinase 6 (CDK6), hepatocyte growth factor receptor (MET), tyrosine-protein kinase ABL1 (ABL1), peroxisome proliferator-activated receptor gamma (PPARG), interleukin-2 (IL2), epidermal growth factor receptor (EGFR), and progesterone receptor (PGR).

The network diagram of "Guava leaf-compound class-active constituents-gene" generated by Cytoscape is shown in Fig. 3, in which the green rectangle shape represents the traditional Chinese medicine guava leaf, and the three pale blue diamond shapes represent sesquiterpene, flavonoids, and triterpenoids; pink ovals represent compounds and yellow hexagons represent genes for the treatment of lung cancer with guava leaves. In the interaction network, the target information corresponding to the compound having a degree value of >20 and the corresponding gene are listed in Table 5.

3.5. GO and KEGG enrichment analysis

Through ClueGO analysis, a total of 1430 GO biological processes were obtained, with 7536 interactions between the biological processes; 35 molecular functions, with 28

Table 1 Molecular information of guava leaf constituents. The first column is the compound name, the second column is the molecular type of the compound, the third column is the number of the constituent, with triterpenoids numbered from T1 to T17, flavonoids from F1 to F30, and sesquiterpenoids from S1 to S19. The molecular formula, the molecular structure, the PubChen ID for compound retrieved from the database and the Pharmmapper JOB ID (the search number of targets in the Pharmmapper database) were listed in the columns four to seven.

Compound Name	Molecular type	Number	Molecular Formula	Molecular structure	PubChem CID	Pharmmapper JOB ID
2α-hydroxyoleanolic acid	Triterpenoid	T1	C30H48O4	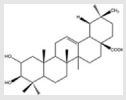	15,560,128	190,417,034,302
3β-O-trans-p-coumaroylmaslinicacid	Triterpenoid	T2	C39H54O5	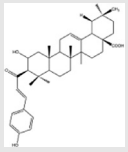	/	190,417,034,505
asiatic acid	Triterpenoid	T3	C30H48O5	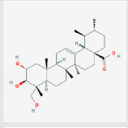	119,034	190,417,034,630
corosolic acid	Triterpenoid	T4	C30H48O4	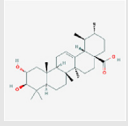	6,918,774	190,417,034,747
goreishic acid I	Triterpenoid	T5	C30H46O4	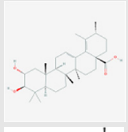	3,081,756	190,318,032,131
guajanoic acid	Triterpenoid	T6	C32H50O6	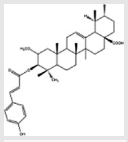	101,211,343	190,417,035,053
guavacoumaric acid	Triterpenoid	T7	C39H54O7	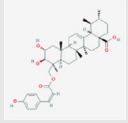	101,211,344	190,417,035,342
guavanoic acid	Triterpenoid	T8	C32H50O6	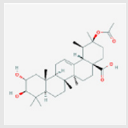	101,211,343	190,417,035,431
ilelatifol D	Triterpenoid	T9	C30H46O4	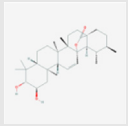	102,572,108	190,318,031,159
isoneriucoumaric acid	Triterpenoid	T10	C39H54O6	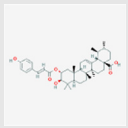	10,100,394	190,417,035,723
jacoumaric acid	Triterpenoid	T11	C39H54O6	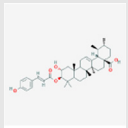	11,700,083	190,417,035,813
obtusinin	Triterpenoid	T12	C15H18O6	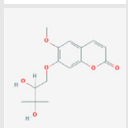	3,604,942	190,318,030,756

(*continued on next page*)

Table 1 (*continued*)

Compound Name	Molecular type	Number	Molecular Formula	Molecular structure	PubChem CID	Pharmmapper JOB ID
obtusol (3β, 27-dihydroxy-urs-12-ene)	Triterpenoid	T13	C30H50O2	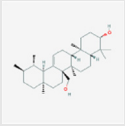	15,895,316	190,417,040,026
oleanolic acid	Triterpenoid	T14	C30H48O3	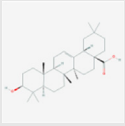	10,494	190,417,040,126
psidiumoic acid	Triterpenoid	T15	C32H50O5	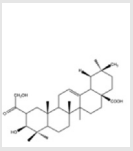	/	190,417,040,228
ursolic acid	Triterpenoid	T16	C30H48O3	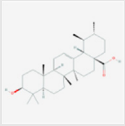	64,945	190,417,040,330
uvoal	Triterpenoid	T17	C30H50O2	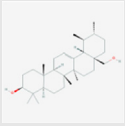	92,802	190,417,040,432
Apigenin	Flavonoid	F1	C15H10O5	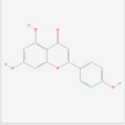	5,280,443	190,414,093,403
Avicularin	Flavonoid	F2	C20H18O11	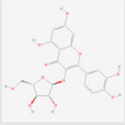	5,490,064	190,414,093,603
Biochanin	Flavonoid	F3	C16H12O5	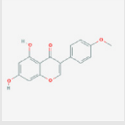	5,280,373	190,403,023,437
Daidzein	Flavonoid	F4	C15H10O4	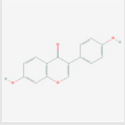	5,281,708	190,414,094,000
demthoxymatteucinol	Flavonoid	F5	C17H16O4	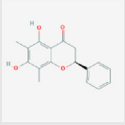	180,550	190,414,094,140
formononetin	Flavonoid	F6	C16H12O4	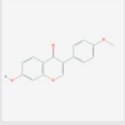	5,280,378	190,414,094,323
Genistein	Flavonoid	F7	C15H10O5	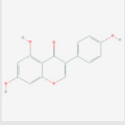	5,280,961	190,414,094,458

Table 1 (*continued*)

Compound Name	Molecular type	Number	Molecular Formula	Molecular structure	PubChem CID	Pharmmapper JOB ID
Genistin	Flavonoid	F8	C21H20O10	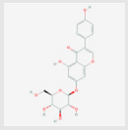	5,281,377	190,414,094,600
Glycitin/daidzin	Flavonoid	F9	C22H22O10	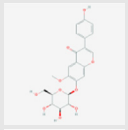	187,808	190,414,094,811
guaijaverin	Flavonoid	F10	C20H18O11	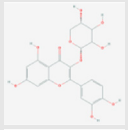	5,481,224	190,414,095,056
guavaric A	Flavonoid	F11	C32H50O6	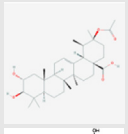	101,211,343	190,414,095,209
guavinoside C	Flavonoid	F12	C27H22O15	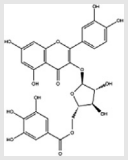	/	190,414,095,324
hyperin	Flavonoid	F13	C21H20O12	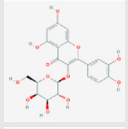	133,568,467	190,417,041,614
isoquercetin(Isoquercitrin)	Flavonoid	F14	C21H20O12	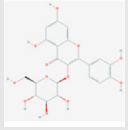	5,280,804	190,414,095,613
kaempferol	Flavonoid	F15	C15H10O6	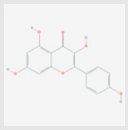	5,280,863	190,414,095,757
kaempferol-3-glucoside	Flavonoid	F16	C21H20O11	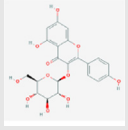	5,282,102	190,414,095,928
Leucocyanidin	Flavonoid	F17	C15H14O7	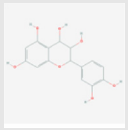	71,629	190,414,100,124
morin-3-O-α-L-lyxopyranoside	Flavonoid	F18	C20H18O11	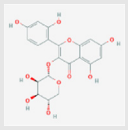	10,455,578	190,414,100,422
myricetin	Flavonoid	F19	C15H10O8	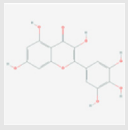	5,281,672	190,414,100,546

(*continued on next page*)

Table 1 (*continued*)

Compound Name	Molecular type	Number	Molecular Formula	Molecular structure	PubChem CID	Pharmmapper JOB ID
Ononin	Flavonoid	F20	C22H22O9	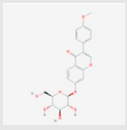	442,813	190,414,100,718
prunetin	Flavonoid	F21	C16H12O5	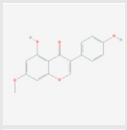	5,281,804	190,414,100,847
quercetin	Flavonoid	F22	C15H10O7	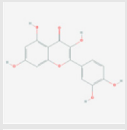	5,280,343	190,414,101,024
quercetin3-O-β-D-xylopyranoside	Flavonoid	F23	C20H18O11	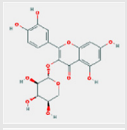	5,320,861	190,414,101,158
quercetin-3-O-(6″-feruloyl) -β-D-galactopyranoside	Flavonoid	F24	C31H28O15	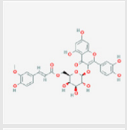	/	190,414,101,321
quercetin-3-O-gentiobioside	Flavonoid	F25	C27H30O17	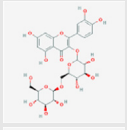	13,915,963	190,414,101,504
quercetin-3-O-β-D-glucuronide	Flavonoid	F26	C21H18O13	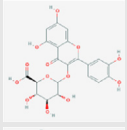	13,258,914	190,414,101,626
quercitrin	Flavonoid	F27	C21H20O11	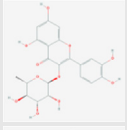	5,280,459	190,414,101,724
reynoutrin	Flavonoid	F28	C20H18O11	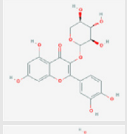	5,320,863	190,414,101,824
rutin	Flavonoid	F29	C27H30O16	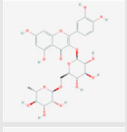	5,280,805	190,414,101,941
xanthone	Flavonoid	F30	C13H8O2	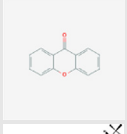	7020	190,414,102,035
Diguajadial	Sesquiterpenoids	S1	C60H66O9	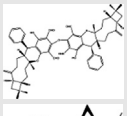	/	190,321,031,034
Guadial A	Sesquiterpenoids	S2	C25H26O5	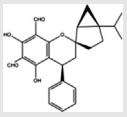	/	190,321,032,624

Table 1 (*continued*)

Compound Name	Molecular type	Number	Molecular Formula	Molecular structure	PubChem CID	Pharmmapper JOB ID
Guadial B	Sesquiterpenoids	S3	C25H26O5	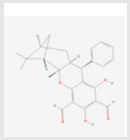	122,377,745	190,319,051,501
Guadial C	Sesquiterpenoids	S4	C25H26O5	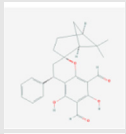	122,377,746	190,319,051,610
Guajadial	Sesquiterpenoids	S5	C30H34O5	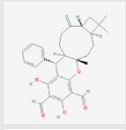	101,447,677	190,318,025,632
Guajadial B	Sesquiterpenoids	S6	C30H34O5	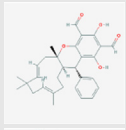	137,346,032	190,319,050,244
Guajadial C	Sesquiterpenoids	S7	C30H34O5	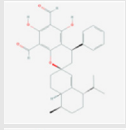	134,714,902	190,319,050,403
Guajadial D	Sesquiterpenoids	S8	C30H34O5	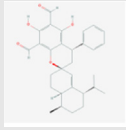	134,714,901	190,319,050,732
Guajadial E	Sesquiterpenoids	S9	C30H34O5	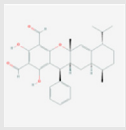	134,714,904	190,319,050,851
Guajadial F	Sesquiterpenoids	S10	C30H34O5	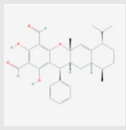	134,714,903	190,319,050,938
Guapsidial A	Sesquiterpenoids	S11	C29H32O5	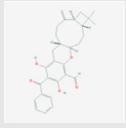	122,377,744	190,319,051,859
Guajadial	Sesquiterpenoids	S12	C30H34O5	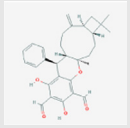	46,197,930	190,320,031,551
Psidial A	Sesquiterpenoids	S13	C30H36O6	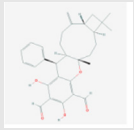	45,104,960	190,318,025,129
Psidial B	Sesquiterpenoids	S14	C30H36O6	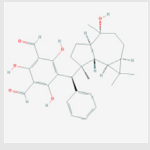	45,104,961	190,318,025,249

(*continued on next page*)

Table 1 (*continued*)

Compound Name	Molecular type	Number	Molecular Formula	Molecular structure	PubChem CID	Pharmmapper JOB ID
Psidial C	Sesquiterpenoids	S15	C30H34O5	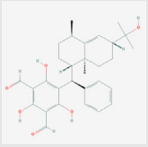	49,844,493	190,318,025,408
Psiguadial A	Sesquiterpenoids	S16	C30H34O5	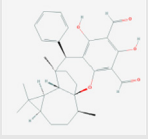	49,844,493	190,318,025,837
Psiguadial B	Sesquiterpenoids	S17	C30H34O5	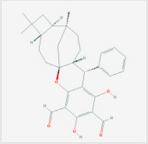	102,052,649	190,318,025,954
Psiguadial C	Sesquiterpenoids	S18	C30H34O6	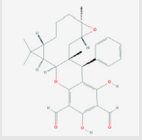	122,224,646	190,319,051,306
Psiguadial D	Sesquiterpenoids	S19	C30H34O5	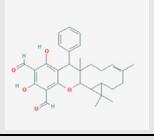	77,984,632	190,321,030,934

Table 2 TCMSP parameter information.

Compound Name	Mol ID	MW	AlogP	Hdon	Hacc	RBN	OB (%)	DL
Apigenin	MOL000008	270.25	2.33	3	5	1	23.06	0.21
Avicularin	MOL007979	434.38	−0.08	7	11	4	2.06	0.7
Daidzein	MOL000390	254.25	2.33	2	4	1	19.44	0.19
formononetin	MOL000392	268.28	2.58	1	4	2	69.67	0.21
Genistein	MOL000481	270.25	2.07	3	5	1	17.93	0.21
Genistin	MOL000480	432.41	0.16	6	10	4	13.35	0.75
daidzin	MOL009720	416.41	0.43	5	9	4	14.32	0.73
guaijaverin	MOL000702	434.38	−0.08	7	11	3	29.65	0.7
hyperin	MOL004368	464.41	−0.59	8	12	4	6.94	0.77
isoquercetin	MOL000437	302.25	0.34	5	7	1	5.92	0.28
kaempferol	MOL000422	286.25	1.77	4	6	1	41.88	0.24
kaempferol-3-glucoside	MOL001415	448.41	−0.32	7	11	4	2.77	0.74
Leucocyanidin	MOL007214	306.29	1.09	6	7	1	37.61	0.27
myricetin	MOL002008	318.25	1.24	6	8	1	13.75	0.31
Ononin	MOL000391	430.44	0.68	4	9	5	11.52	0.78
prunetin	MOL000486	284.28	2.32	2	5	2	5.41	0.24
quercetin	MOL000098	302.25	1.5	5	7	1	46.43	0.28
quercetin-3-O-β-D-glucuronide	MOL001001	450.38	−0.42	8	12	3	30.66	0.74
quercitrin	MOL000701	448.41	0.3	7	11	3	4.04	0.74
rutin	MOL000415	610.57	−1.45	10	16	6	3.2	0.68
2α-hydroxyoleanolic acid	MOL012969	471.77	4.78	2	4	1	17.38	0.74
asiatic acid	MOL006861	488.78	4.41	4	5	2	16.69	0.72
oleanolic acid	MOL000263	456.78	6.42	2	3	1	29.02	0.76
ursolic acid	MOL000511	456.78	6.47	2	3	1	16.77	0.75
olmelin	MOL000510	284.28	2.32	2	5	2	25.21	0.24

interactions between the molecular functions; and 203 GO cell components, with 470 interactions between the cell components. KEGG analysis was performed by KOBAS 3.0, and 217 pathway enrichment results were obtained. GO analysis results of the interacting genes between guava leaves and lung cancer are shown in Table 6.

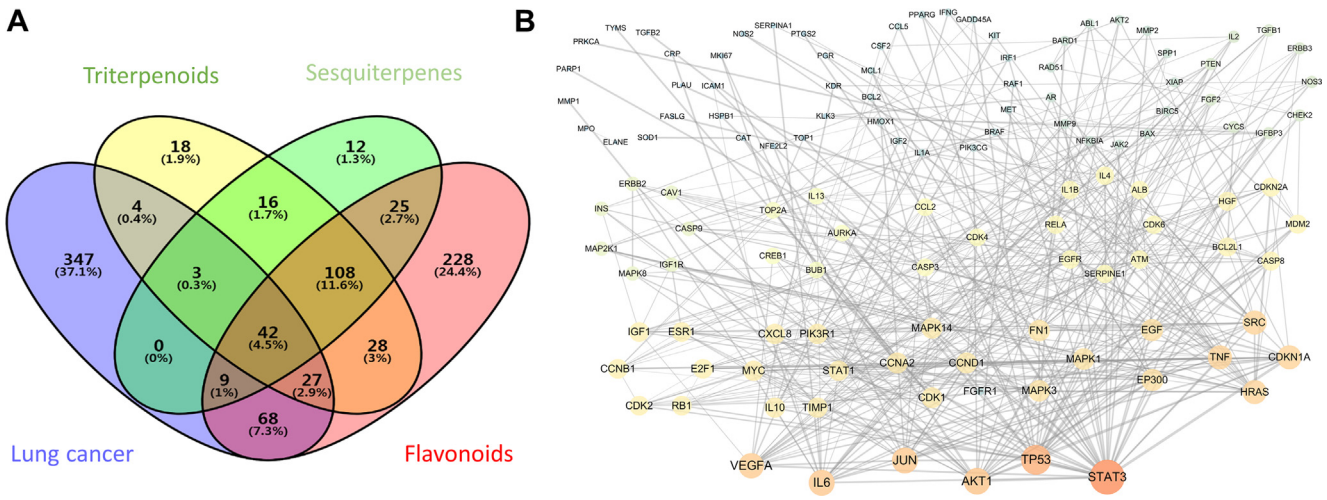

Fig. 2 Drug-disease interaction network analysis (A) Screening of guava leaf-lung cancer common gene. (B) Topological analysis of drug-disease interactive gene network.

Table 3 Topology analysis data of drug-disease interaction gene (Degree $\geq$ 10).

Gene	Full Name	Degree	Uniprot ID	Protein class
STAT3	signal transducer and activator of transcription 3	35	P40763	nucleic acid binding; transcription factor
TP53	tumor protein p53	27	P04637	transcription factor
AKT1	AKT serine/threonine kinase 1	22	P31749	calcium-binding protein; kinase; transferase; transfer/carrierprotein
IL6	interleukin 6	21	P05231	None
JUN	Transcription factor AP-1	21	P05412	nucleic acid binding; transcription factor
VEGFA	vascular endothelial growth factor A	20	P15692	signaling molecule
SRC	non-receptor tyrosine kinase	18	P12931	None
TNF	tumor necrosis factor	18	P01375	signaling molecule
HRAS	HRas proto-oncogene, GTPase	18	P01112	enzyme modulator
CDKN1A	cyclin dependent kinase inhibitor 1A	18	P38936	None
EGF	epidermal growth factor	15	P01133	None
EP300	E1A binding protein p300	15	Q09472	nucleic acid binding; transcription factor; transferase
FN1	fibronectin 1	14	P02751	signaling molecule
MAPK3	mitogen-activated protein kinase 3	14	P27361	kinase; transferase
MAPK1	mitogen-activated protein kinase 1	14	P28482	kinase; transferase
MAPK14	mitogen-activated protein kinase 14	13	Q16539	kinase; transferase
CCNA2	cyclin A2	13	P20248	enzyme modulator
CDK1	cyclin dependent kinase 1	13	P06493	kinase; transferase
CCND1	cyclin D1	13	P24385	enzyme modulator
PIK3R1	phosphoinositide-3-kinase regulatory subunit 1	12	P27986	enzyme modulator
CXCL8	C-X-C motif chemokine ligand 8	12	P10145	signaling molecule
MYC	MYC proto-oncogene	12	P01106	nucleic acid binding; transcription factor
IL10	interleukin 10	12	P22301	None
TIMP1	TIMP metallopeptidase inhibitor 1	12	P01033	enzyme modulator
STAT1	signal transducer and activator of transcription 1	12	P42224	nucleic acid binding; transcription factor
ESR1	estrogen receptor 1	11	P03372	nucleic acid binding; receptor; transcription factor
IGF1	insulin like growth factor 1	11	P05019	None
CCNB1	cyclin B1	11	P14635	enzyme modulator
CDK2	cyclin dependent kinase 2	11	P24941	kinase; transferase
RB1	RB transcriptional corepressor 1	11	P06400	nucleic acid binding; transcription factor
E2F1	E2F transcription factor 1	11	Q01094	nucleic acid binding; transcription factor
CDKN2A	cyclin dependent kinase inhibitor 2A	10	P42771	None
HGF	hepatocyte growth factor	10	P14210	hydrolase; protease
BCL2L1	BCL2 like 1	10	Q07817	signaling molecule
CASP8	caspase 8	10	Q14790	enzyme modulator; hydrolase; protease
MDM2	MDM2 proto-oncogene	10	Q00987	nucleic acid binding

Table 4 Interaction network data of "guava leaf – compound class – active component – gene"(Degree ≥ 20).

Node Name	Degree	Average Shortest Path Length	Closeness Centrality	Radiality
quercetin	85	1.96396396	0.50917431	0.80720721
genistein	62	2.15315315	0.46443515	0.76936937
apigenin	53	2.22522523	0.44939271	0.75495495
ursolic acid	43	2.31531532	0.43190661	0.73693694
daidzein	38	2.37837838	0.42045455	0.72432432
kaempferol	33	2.45045045	0.40808824	0.70990991
myricetin	30	2.45045045	0.40808824	0.70990991
rutin	22	2.6036036	0.38408304	0.67927928
formononetin	21	2.53153153	0.39501779	0.69369369
demthoxymatteucinol	21	2.51351351	0.39784946	0.6972973
Guadial B	20	2.56756757	0.38947368	0.68648649
VDR	36	2.44594595	0.40883978	0.71081081
CDK2	29	2.31981982	0.43106796	0.73603604
MAP2K1	27	2.6981982	0.3706177	0.66036036
CDK6	26	2.18468468	0.45773196	0.76306306
MET	25	2.90540541	0.34418605	0.61891892
ABL1	24	2.42792793	0.41187384	0.71441441
PPARG	22	2.28378378	0.43786982	0.74324324
IL2	22	2.37387387	0.42125237	0.72522523
EGFR	22	2.3018018	0.43444227	0.73963964
PGR	21	2.40990991	0.41495327	0.71801802
MAPK14	21	2.58108108	0.38743455	0.68378378
KIT	21	2.77927928	0.35980551	0.64414414
RARB	20	2.77927928	0.35980551	0.64414414
NOS2	20	2.53603604	0.39431616	0.69279279

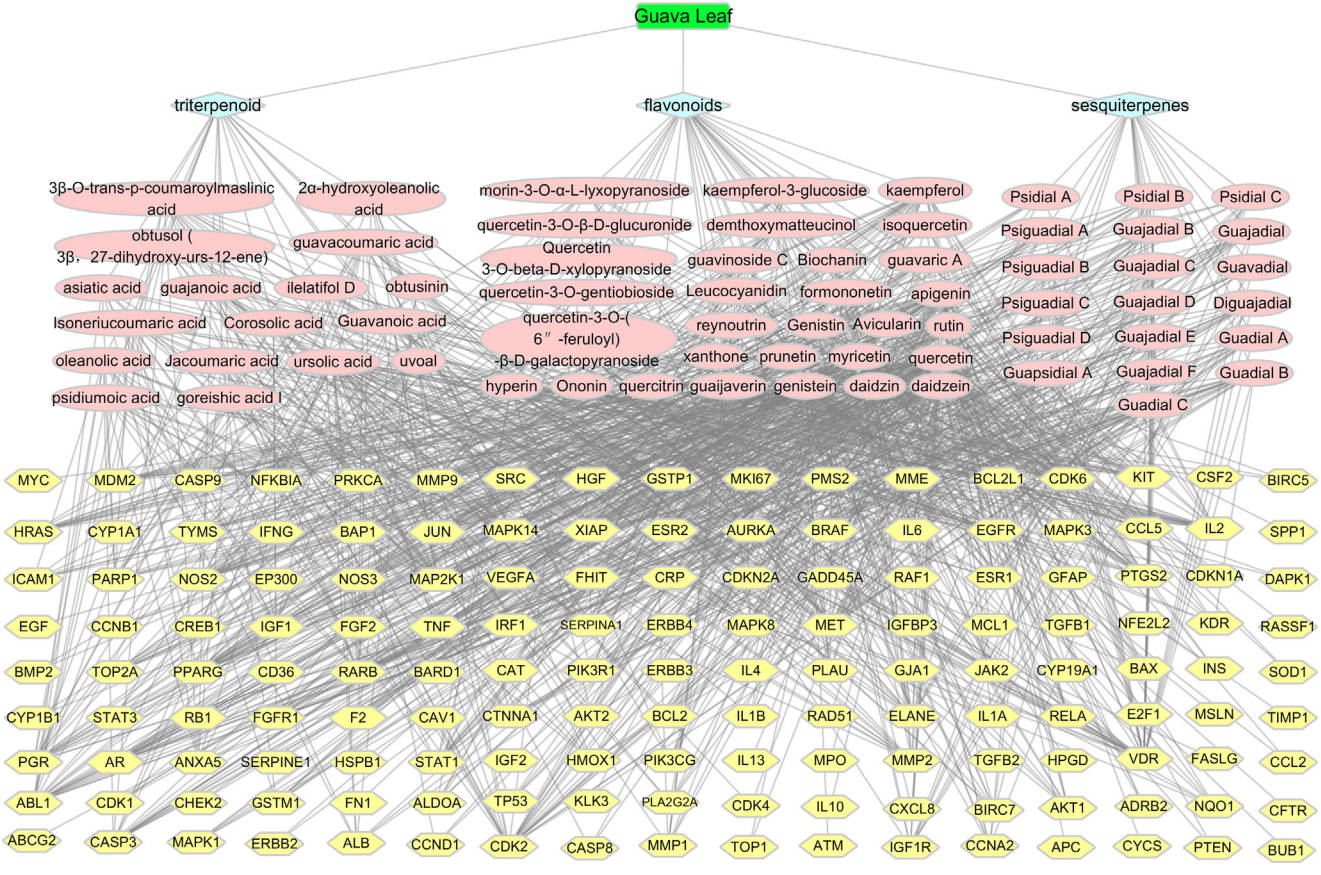

Fig. 3 Interactive network of 'guava leaf - compound class – active compound – gene'.

Table 5 Target and genetic information of compounds with interaction network Degree $\geq$ 20.

Compound	Targets	Genes
apigenin	RAC-alpha serine/threonine-protein kinase	AKT1
apigenin	Adenomatous polyposis coli protein	APC
apigenin	Androgen receptor	AR
apigenin	Apoptosis regulator BAX	BAX
apigenin	Apoptosis regulator Bcl-2	BCL2
apigenin	Bcl-2-like protein 1	BCL2L1
apigenin	Caspase-3	CASP3
apigenin	Caspase-9	CASP9
apigenin	G2/mitotic-specific cyclin-B1	CCNB1
apigenin	G1/S-specific cyclin-D1	CCND1
apigenin	Cell division control protein 2 homolog	CDK1
apigenin	Cell division protein kinase 2	CDK2
apigenin	Cell division protein kinase 4	CDK4
apigenin	Cell division protein kinase 6	CDK6
apigenin	Cyclin-dependent kinase inhibitor 1	CDKN1A
apigenin	Cyclin-dependent kinase inhibitor 2	CDKN2A
apigenin	Cytochrome *c*	CYCS
apigenin	Cytochrome P450 19A1	CYP19A1
apigenin	Estrogen receptor	ESR1
apigenin	Estrogen receptor beta	ESR2
apigenin	Prothrombin	F2
apigenin	Basic fibroblast growth factor receptor 1	FGFR1
apigenin	Heme oxygenase 1	HMOX1
apigenin	Intercellular adhesion molecule 1	ICAM1
apigenin	Interferon gamma	IFNG
apigenin	Insulin-like growth factor 1 receptor	IGF1R
apigenin	Interleukin-13	IL13
apigenin	Interleukin-2	IL2
apigenin	Interleukin-4	IL4
apigenin	Insulin	INS
apigenin	Transcription factor AP-1	JUN
apigenin	Vascular endothelial growth factor receptor 2	KDR
apigenin	Induced myeloid leukemia cell differentiation protein Mcl-1	MCL1
apigenin	E3 ubiquitin-protein ligase Mdm2	MDM2
apigenin	Interstitial collagenase	MMP1
apigenin	Matrix metalloproteinase-9	MMP9
apigenin	NF-kappa-B inhibitor alpha	NFKBIA
apigenin	Nitric oxide synthase, endothelial	NOS3
apigenin	Phosphatidylinositol-4,5-bisphosphate 3-kinase catalytic subunit, gamma isoform	PIK3CG
apigenin	Phospholipase A2, membrane associated	PLA2G2A
apigenin	Urokinase-type plasminogen activator	PLAU
apigenin	Prostaglandin G/H synthase 2	PTGS2
apigenin	Retinoblastoma-associated protein	RB1
apigenin	Transcription factor p65	RELA
apigenin	Alpha-1-antitrypsin	SERPINE1
apigenin	Proto-oncogene tyrosine-protein kinase Src	SRC
apigenin	Tumor necrosis factor	TNF
apigenin	DNA topoisomerase II	TOP2A
apigenin	Cellular tumor antigen p53	TP53
apigenin	Vitamin D3 receptor	VDR
apigenin	Vascular endothelial growth factor A	VEGFA
apigenin	Baculoviral IAP repeat-containing protein 4	XIAP
daidzein	Beta-2 adrenergic receptor	ADRB2
daidzein	Ubiquitin carboxyl-terminal hydrolase BAP1	BAP1
daidzein	BRCA1-associated RING domain protein 1	BARD1
daidzein	Apoptosis regulator BAX	BAX
daidzein	Caspase-3	CASP3
daidzein	Catalase	CAT
daidzein	Caveolin-1	CAV1
daidzein	Cell division protein kinase 2	CDK2
daidzein	Cell division protein kinase 6	CDK6
daidzein	Cyclin-dependent kinase inhibitor 1	CDKN1A
daidzein	Histone acetyltransferase p300	EP300

(*continued on next page*)

Table 5 (*continued*)

Compound	Targets	Genes
daidzein	Estrogen receptor	ESR1
daidzein	Estrogen receptor beta	ESR2
daidzein	Prothrombin	F2
daidzein	Growth arrest and DNA damage-inducible protein GADD45 alpha	GADD45A
daidzein	Intercellular adhesion molecule 1	ICAM1
daidzein	Insulin-like growth factor 1 receptor	IGF1R
daidzein	Interleukin-4	IL4
daidzein	Interleukin-6	IL6
daidzein	Transcription factor AP-1	JUN
daidzein	Mitogen-activated protein kinase 14	MAPK14
daidzein	Mitogen-activated protein kinase 8	MAPK8
daidzein	Antigen KI-67	MKI67
daidzein	Neprilysin	MME
daidzein	Nitric oxide synthase, inducible	NOS2
daidzein	Nitric oxide synthase, endothelial	NOS3
daidzein	Progesterone receptor	PGR
daidzein	Phosphatidylinositol 3-kinase regulatory subunit alpha	PIK3R1
daidzein	Peroxisome proliferator activated receptor gamma	PPARG
daidzein	Peroxisome proliferator activated receptor gamma	PPARG
daidzein	Prostaglandin G/H synthase 2	PTGS2
daidzein	DNA repair protein RAD51 homolog 1	RAD51
daidzein	Transcription factor p65	RELA
daidzein	Signal transducer and activator of transcription 1-alpha/beta	STAT1
daidzein	Tumor necrosis factor	TNF
daidzein	Cellular tumor antigen p53	TP53
daidzein	Vascular endothelial growth factor A	VEGFA
demthoxymatteucinol	Proto-oncogene tyrosine-protein kinase ABL1	ABL1
demthoxymatteucinol	Serine/threonine-protein kinase 6	AURKA
demthoxymatteucinol	Bone morphogenetic protein 2	BMP2
demthoxymatteucinol	Cell division protein kinase 6	CDK6
demthoxymatteucinol	Catenin alpha-1	CTNNA1
demthoxymatteucinol	Leukocyte elastase	ELANE
demthoxymatteucinol	Basic fibroblast growth factor receptor 1	FGFR1
demthoxymatteucinol	Insulin-like growth factor 1 receptor	IGF1R
demthoxymatteucinol	Tyrosine-protein kinase JAK2	JAK2
demthoxymatteucinol	Vascular endothelial growth factor receptor 2	KDR
demthoxymatteucinol	Mast/stem cell growth factor receptor	KIT
demthoxymatteucinol	Dual specificity mitogen-activated protein kinase kinase 1	MAP2K1
demthoxymatteucinol	Nitric oxide synthase, endothelial	NOS3
demthoxymatteucinol	NAD(P)H dehydrogenase [quinone] 1	NQO1
demthoxymatteucinol	Progesterone receptor	PGR
demthoxymatteucinol	Phospholipase A2, membrane associated	PLA2G2A
demthoxymatteucinol	Urokinase-type plasminogen activator	PLAU
demthoxymatteucinol	Peroxisome proliferator activated receptor gamma	PPARG
demthoxymatteucinol	Thymidylate synthase	TYMS
demthoxymatteucinol	Vitamin D3 receptor	VDR
formononetin	Beta-2 adrenergic receptor	ADRB2
formononetin	Androgen receptor	AR
formononetin	C-C motif chemokine 5	CCL5
formononetin	Cyclin-A2	CCNA2
formononetin	Cell division protein kinase 2	CDK2
formononetin	Cell division protein kinase 6	CDK6
formononetin	Estrogen receptor	ESR1
formononetin	Estrogen receptor beta	ESR2
formononetin	Prothrombin	F2
formononetin	Interleukin-4	IL4
formononetin	Transcription factor AP-1	JUN
formononetin	Mitogen-activated protein kinase 14	MAPK14
formononetin	Mitogen-activated protein kinase 8	MAPK8
formononetin	Neprilysin	MME
formononetin	Nitric oxide synthase, inducible	NOS2
formononetin	Nitric oxide synthase, endothelial	NOS3
formononetin	Progesterone receptor	PGR

Table 5 (*continued*)

Compound	Targets	Genes
formononetin	Peroxisome proliferator activated receptor gamma	PPARG
formononetin	Peroxisome proliferator activated receptor gamma	PPARG
formononetin	Prostaglandin G/H synthase 2	PTGS2
genistein	RAC-alpha serine/threonine-protein kinase	AKT1
genistein	Androgen receptor	AR
genistein	Serine-protein kinase ATM	ATM
genistein	Apoptosis regulator BAX	BAX
genistein	Apoptosis regulator Bcl-2	BCL2
genistein	Baculoviral IAP repeat-containing protein 5	BIRC5
genistein	Baculoviral IAP repeat-containing protein 7	BIRC7
genistein	Mitotic checkpoint serine/threonine-protein kinase BUB1	BUB1
genistein	Caspase-3	CASP3
genistein	Caspase-9	CASP9
genistein	C-C motif chemokine 2	CCL2
genistein	Cyclin-A2	CCNA2
genistein	G2/mitotic-specific cyclin-B1	CCNB1
genistein	Cell division control protein 2 homolog	CDK1
genistein	Cell division protein kinase 2	CDK2
genistein	Cyclin-dependent kinase inhibitor 1	CDKN1A
genistein	Cyclin-dependent kinase inhibitor 2	CDKN2A
genistein	Cystic fibrosis transmembrane conductance regulator	CFTR
genistein	Serine/threonine-protein kinase Chk2	CHEK2
genistein	Interleukin-8	CXCL8
genistein	Epidermal growth factor receptor	EGFR
genistein	Leukocyte elastase	ELANE
genistein	Receptor tyrosine-protein kinase erbB-2	ERBB2
genistein	Estrogen receptor	ESR1
genistein	Estrogen receptor beta	ESR2
genistein	Prothrombin	F2
genistein	Basic fibroblast growth factor receptor 1	FGFR1
genistein	Fibronectin	FN1
genistein	Glial fibrillary acidic protein	GFAP
genistein	15-hydroxyprostaglandin dehydrogenase [NAD +]	HPGD
genistein	Intercellular adhesion molecule 1	ICAM1
genistein	Insulin-like growth factor 1 receptor	IGF1R
genistein	Interleukin-1 beta	IL1B
genistein	Insulin	INS
genistein	Transcription factor AP-1	JUN
genistein	Prostate-specific antigen	KLK3
genistein	Mitogen-activated protein kinase 1	MAPK1
genistein	Mitogen-activated protein kinase 14	MAPK14
genistein	Mitogen-activated protein kinase 3	MAPK3
genistein	E3 ubiquitin-protein ligase Mdm2	MDM2
genistein	Neprilysin	MME
genistein	Matrix metalloproteinase-9	MMP9
genistein	Mesothelin	MSLN
genistein	Nitric oxide synthase, inducible	NOS2
genistein	Nitric oxide synthase, endothelial	NOS3
genistein	Progesterone receptor	PGR
genistein	Phosphatidylinositol-4,5-bisphosphate 3-kinase catalytic subunit, gamma isoform	PIK3CG
genistein	Urokinase-type plasminogen activator	PLAU
genistein	Peroxisome proliferator activated receptor gamma	PPARG
genistein	Peroxisome proliferator activated receptor gamma	PPARG
genistein	Phosphatidylinositol-3,4,5-trisphosphate 3-phosphatase and dual-specificity protein phosphatase PTEN	PTEN
genistein	Prostaglandin G/H synthase 2	PTGS2
genistein	Transcription factor p65	RELA
genistein	Signal transducer and activator of transcription 1-alpha/beta	STAT1
genistein	Signal transducer and activator of transcription 3	STAT3
genistein	Transforming growth factor beta-1	TGFB1
genistein	Transforming growth factor beta-2	TGFB2
genistein	Metalloproteinase inhibitor 1	TIMP1
genistein	Tumor necrosis factor	TNF
genistein	Cellular tumor antigen p53	TP53
genistein	Vascular endothelial growth factor A	VEGFA

The top 10 enriched biological processes are shown in Fig. 4A. The enrichment results included apoptosis, programmed cell death, regulation of programmed cell death, regulation of cell death, regulation of apoptotic process, regulation of cell population proliferation, response to oxygen-containing compound, negative regulation of programmed cell death, and negative regulation of cell death. The top 10 enriched cellular components are shown in

Table 6 GO enrichment analysis of the "guava leaf-lung cancer" interaction gene.

GO ID	GO Term	Percentage of genes	P-Value	Corr P-Value
GO:0006915	apoptotic process(BP)	112/2458 (4.56%)	9.13E−64	1.18E−60
GO:0012501	programmed cell death (BP)	114/2605(4.38%)	1.59E−63	2.05E−60
GO:0043067	regulation of programmed cell death (BP)	103/1991(5.17%)	4.85E−62	6.24E−59
GO:0010941	regulation of cell death(BP)	105/2153(4.88%)	4.24E−61	5.45E−58
GO:0042981	regulation of apoptotic process(BP)	101/1971(5.12%)	5.21E−60	6.69E−57
GO:0042127	regulation of cell population proliferation(BP)	100/2092(4.78%)	2.59E−56	3.32E−53
GO:1901700	response to oxygen-containing compound(BP)	98/2088(4.69%)	4.63E−54	5.94E−51
GO:0051247	positive regulation of protein metabolic process(BP)	97/2115(4.59%)	2.12E−52	2.72E−49
GO:0043069	negative regulation of programmed cell death(BP)	78/1182(6.60%)	2.21E−51	2.83E−48
GO:0060548	negative regulation of cell death(BP)	78/1299(6.16%)	1.23E−50	1.58E−47
GO:0031093	platelet alpha granule lumen(CC)	15/88(17.05%)	3.46E−16	1.14E−14
GO:0031091	platelet alpha granule(CC)	16/118(13.56%)	1.51E−15	4.83E−14
GO:0031983	vesicle lumen(CC)	24/470(5.11%)	4.76E−13	1.48E−11
GO:0060205	cytoplasmic vesicle lumen(CC)	23/469(4.90%)	3.51E−12	1.05E−10
GO:0034774	secretory granule lumen(CC)	22/448(4.91%)	1.05E−11	3.06E−10
GO:0000307	cyclin-dependent protein kinase holoenzyme complex(CC)	10/57(17.54%)	2.54E−11	7.12E−10
GO:0045121	membrane raft(CC)	21/441(4.76%)	5.74E−11	1.55E−09
GO:0098857	membrane microdomain(CC)	21/442(4.75%)	5.98E−11	1.56E−09
GO:0098589	membrane region(CC)	21/457(4.60%)	1.11E−10	2.77E−09
GO:1902911	protein kinase complex(CC)	11/137(8.03%)	1.36E−08	3.26E−07
GO:0004672	protein kinase activity(MF)	72/1534(4.69%)	1.14E−36	2.51E−34
GO:0043085	positive regulation of catalytic activity(MF)	76/1809(4.20%)	9.45E−36	2.07E−33
GO:0016773	phosphotransferase activity, alcohol group as acceptor(MF)	73/1661(4.39%)	2.32E−35	5.06E−33
GO:0016301	kinase activity(MF)	75/1798(4.17%)	5.68E−35	1.23E−32
GO:0004674	protein serine/threonine kinase activity(MF)	60/1094(5.48%)	1.79E−33	3.87E−31
GO:0051338	regulation of transferase activity(MF)	64/1298(4.93%)	3.03E−33	6.51E−31
GO:0043549	regulation of kinase activity(MF)	61/1153(5.29%)	3.28E−33	7.01E−31
GO:0071900	regulation of protein serine/threonine kinase activity(MF)	50/708(7.06%)	1.36E−32	2.89E−30
GO:0045859	regulation of protein kinase activity(MF)	58/1067(5.44%)	4.95E−32	1.05E−29
GO:0033674	positive regulation of kinase activity(MF)	50/7755(6.45%)	9.88E−31	2.08E−28

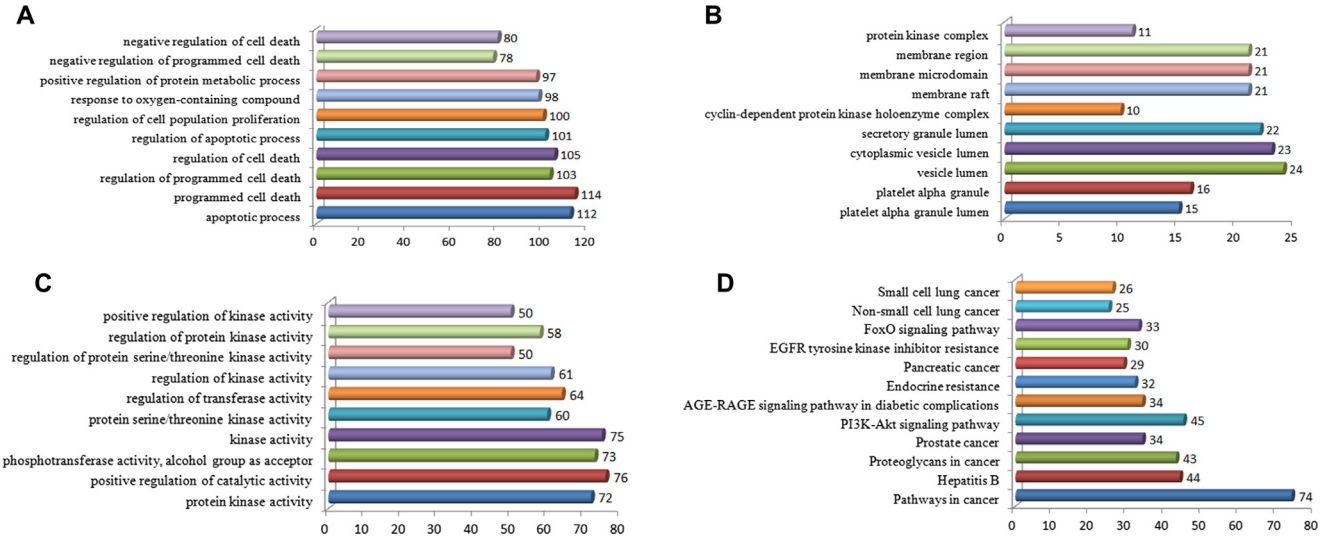

Fig. 4 GO and KEGG analysis of 'guava leaf – lung cancer' interactive gene with P-values from small to large. (A) GO biological process analysis of 'guava leaf – lung cancer' interactive gene with P-values from small to large. (B) GO cell components analysis of 'guava leaf – lung cancer' interactive gene with P-values from small to large. (C) GO molecular function analysis of 'guava leaf – lung cancer' interactive gene with P-values from small to large. (D) KEGG analysis of 'guava leaf – lung cancer' cross-gene.

Fig. 4B. The enrichment results included platelet alpha granule lumen, platelet alpha granules, vesicle lumen, cytoplasmic vesicle lumen, secretory granule lumen, cyclin-dependent protein kinase holoenzyme complex, membrane raft, membrane microdomain, membrane region, and protein kinase complex. The top 10 enriched molecular function terms are shown in Fig. 4C. The enrichment results included protein kinase activity, positive regulation of catalytic activity, phosphotransferase activity, alcohol group as acceptor, phosphokinase activity, kinase activity, protein serine/threonine kinase activity, regulation of transferase activity, regulation of kinase activity, regulation of protein serine/threonine kinase activity, regulation of protein kinase activity, and positive regulation of kinase activity.

KEGG enrichment analysis results of common genes between guava leaf constituent target and lung cancer related genes are shown in Fig. 4D, Table 7 and Table 8. The top 10 common enriched pathways are listed below: cancer path-

Table 7 Results of KEGG enrichment analysis of "guava leaf-lung cancer" interactive gene.

KEGG ID	GO Term	Percentage of genes	P-Value	Corr P-Value
hsa05200	Pathways in cancer	74/397(18.64%)	1.63E−101	3.53E−99
hsa05161	Hepatitis B	44/146(30.14%)	1.06E−66	1.15E−64
hsa05205	Proteoglycans in cancer	43/205(20.98%)	3.33E−59	2.41E−57
hsa05215	Prostate cancer	34/89(38.20%)	2.56E−54	1.39E−52
hsa04151	PI3K-Akt signaling pathway	45/342(13.16%)	9.08E−54	3.94E−52
hsa04933	AGE-RAGE signaling pathway in diabetic complications	34/101(33.66%)	9.60E−53	3.47E−51
hsa01522	Endocrine resistance	32/97 (32.99%)	2.15E−49	6.68E−48
hsa05212	Pancreatic cancer	29/66(43.94%)	8.75E−48	2.37E−46
hsa01521	EGFR tyrosine kinase inhibitor resistance	30/81(37.04%)	1.39E−47	3.35E−46
hsa04068	FoxO signaling pathway	33/134(24.63%)	2.60E−47	5.64E−46
hsa05223	Non-small cell lung cancer	25/56(44.64%)	2.17E−41	3.63E−40
hsa05222	Small cell lung cancer	26/86(30.23%)	2.45E−39	2.95E−38

Table 8 The enrichment gene list of KEGG of "guava leaf - lung cancer" interaction gene.

KEGG ID	Enriched genes in the KEGG pathway
hsa05200	CCND1,BCL2,BCL2L1,PIK3CG,TGFB2,XIAP,KIT,BIRC5,MAP2K1,PTGS2,NOS2,JUN,RAD51,ABL1,PTEN,CASP3,TP53, GSTP1,CXCL8,DAPK1,IGF1,RB1,EP300,CDK4,BMP2,AKT2,CDK6,FGFR1,FGF2,TGFB1,HGF,MMP1,MMP2,RASSF1, APC,AKT1,BAX,MMP9,IGF1R,CYCS,BIRC7,BRAF,MDM2,EGFR,RAF1,EGF,MYC,E2F1,PPARG,MET,STAT3, NFKBIA,FN1,CDKN1A,MAPK3,MAPK1,CASP8,PRKCA,MAPK8,ERBB2,IL6,CDKN2A,STAT1,FASLG,KLK3,CDK2, VEGFA,AR,RARB,HRAS,RELA,PIK3R1,CASP9,CTNNA1
hsa05161	CCND1,BCL2,PIK3CG,TGFB2,BIRC5,MAP2K1,JUN,TNF,PTEN,CASP3,TP53,CXCL8,RB1,EP300,CDK4,CDK2,CCNA2, PIK3R1,AKT1,BAX,MMP9,AKT2,CYCS,RAF1,TGFB1,MYC,E2F1,CDK6,SRC,STAT3,NFKBIA,CASP9,CDKN1A, MAPK3,MAPK1,CASP8,PRKCA,MAPK8,IL6,STAT1,FASLG,HRAS,RELA,CREB1
hsa05205	CCND1,PIK3CG,MYC,MAP2K1,ESR1,TNF,CAV1,CASP3,TP53,KDR,IGF1,MMP9,AKT2,FGFR1,FGF2,HGF,MMP2, AKT1,IGF2,IGF2,IGF1R,MDM2,BRAF,EGFR,RAF1,TGFB1,TGFB2,MAPK14,SRC,MET,PLAU,FN1,CDKN1A,MAPK3, MAPK1,PRKCA,STAT3,ERBB2,FASLG,VEGFA,HRAS,PIK3R1,ERBB3,ERBB4
hsa05215	CDK2,CDKN1A,CREB1,E2F1,EGF,EGFR,EP300,ERBB2,AKT1,AKT2,FGFR1,GSTP1,HRAS,IGF1,IGF1R,KLK3,INS,AR, MDM2,NFKBIA,PIK3CG,PIK3R1,MAPK1,MAPK3,MAP2K1,PTEN,RAF1,RB1,CCND1,BCL2,RELA,BRAF,TP53,CASP9
hsa04151	CDK2,CDK4,CDK6,CDKN1A,CREB1,EGF,EGFR,AKT1,AKT2,FGF2,FGFR1,FN1,HGF,HRAS,IGF1,IGF1R,IL2,FASLG, IL4,IL6,INS,JAK2,KDR,KIT,MCL1,MDM2,MET,MYC,NOS3,PIK3CG,PIK3R1,PRKCA,MAPK1,MAPK3,MAP2K1,PTEN, RAF1,CCND1,BCL2,RELA,BCL2L1,SPP1,TP53,VEGFA,CASP9
hsa04933	CDK4,MAPK14,AKT1,AKT2,FN1,HRAS,ICAM1,IL1A,IL1B,IL6,CXCL8,JAK2,JUN,MMP2,NOS3,SERPINE1,PIK3CG, PIK3R1,PRKCA,MAPK1,MAPK3,MAPK8,BAX,CCND1,BCL2,RELA,CCL2,STAT1,STAT3,TGFB1,TGFB2,TNF,VEGFA, CASP3
hsa01522	CDK4,CDKN1A,CDKN2A,MAPK14,E2F1,EGFR,ERBB2,AKT1,AKT2,ESR1,ESR2,HRAS,IGF1,IGF1R,JUN,MDM2, MMP2,MMP9,PIK3CG,PIK3R1,MAPK1,MAPK3,MAPK8,MAP2K1,BAX,RAF1,RB1,CCND1,BCL2,SRC,BRAF,TP53
hsa05212	CDK4,CDK6,CDKN2A,E2F1,EGF,EGFR,ERBB2,AKT1,AKT2,PIK3CG,PIK3R1,MAPK1,MAPK3,MAPK8,MAP2K1, RAD51,RAF1,RB1,CCND1,RELA,BCL2L1,BRAF,STAT1,STAT3,TGFB1,TGFB2,TP53,VEGFA,CASP9
hsa01521	EGF,EGFR,ERBB2,ERBB3,AKT1,AKT2,FGF2,HGF,HRAS,IGF1,IGF1R,IL6,JAK2,KDR,MET,PIK3CG,PIK3R1,PRKCA, MAPK1,MAPK3,MAP2K1,PTEN,BAX,RAF1,BCL2,BCL2L1,SRC,BRAF,STAT3,VEGFA
hsa04068	CDK2,CDKN1A,MAPK14,GADD45A,EGF,EGFR,EP300,AKT1,AKT2,HRAS,IGF1,IGF1R,FASLG,IL6,IL10,INS,MDM2, ATM,PIK3CG,PIK3R1,MAPK1,MAPK3,MAPK8,MAP2K1,PTEN,RAF1,CCND1,BRAF,STAT3,TGFB1,TGFB2,CAT, CCNB1
hsa05223	CDK4,CDK6,CDKN2A,RASSF1,E2F1,EGF,EGFR,ERBB2,AKT1,AKT2,FHIT,HRAS,PIK3CG,PIK3R1,PRKCA,MAPK1, MAPK3,MAP2K1,RAF1,RARB,RB1,CCND1,BRAF,TP53,CASP9
hsa05222	CDK2,CDK4,CDK6,E2F1,AKT1,AKT2,FHIT,FN1,XIAP,MYC,NFKBIA,NOS2,PIK3CG,PIK3R1,CYCS,PTEN,PTGS2, RARB,RB1,CCND1,BCL2,RELA,BCL2L1,TP53,BIRC7,CASP9

way, hepatitis B, proteoglycans in cancer, prostate cancer, PI3K-Akt signaling pathway, AGE-RAGE signaling pathway in diabetic complications, endocrine resistance, pancreatic cancer, EGFR tyrosine kinase inhibitor resistance, and FoxO signaling pathway. The non-small cell lung cancer and small cell lung cancer pathways were also recorded.

One of these pathways is the PI3K-Akt signaling pathway, which has been shown to play an important regulatory role in tumor therapy. The PI3K-Akt signaling pathway is an important pathway for cell survival, metabolism, angiogenesis, apoptosis, proliferation and differentiation. The substrate is used to control key cellular processes, and many targets are involved in this pathway and AKT also plays an important role in the regulation of this pathway (Ebrahimi et al., 2017). In order to investigate the effectiveness of guava leaf constituents on lung cancer via the PI3K-Akt signaling pathway, we analyzed the expression (Fig. 5A) and the pathway activities (Fig. 5) of these genes in lung squamous cell carcinoma (LUSC) and lung adenocarcinoma (LUAD) samples from TCGA database in the GSCAlite online platform. The results indicated that the PI3K-Akt signaling pathway genes that could be potentially affected by the guava leaf constituents showed differential expression with some of them being downregulated (Fig. 5A, blue color dot) or upregulated (Fig. 5A, red color dot) in both LUSC and LUAD. In addition, we found that some of the target genes of the guava leaf constituents did not show differential expression in lung cancer (Fig. 5A). Furthermore, in pathway activity analysis, we found that these target genes were involved in the inhibition or activation of important pathways such as PI3K-Akt, apoptosis, cell cycle, EMT,

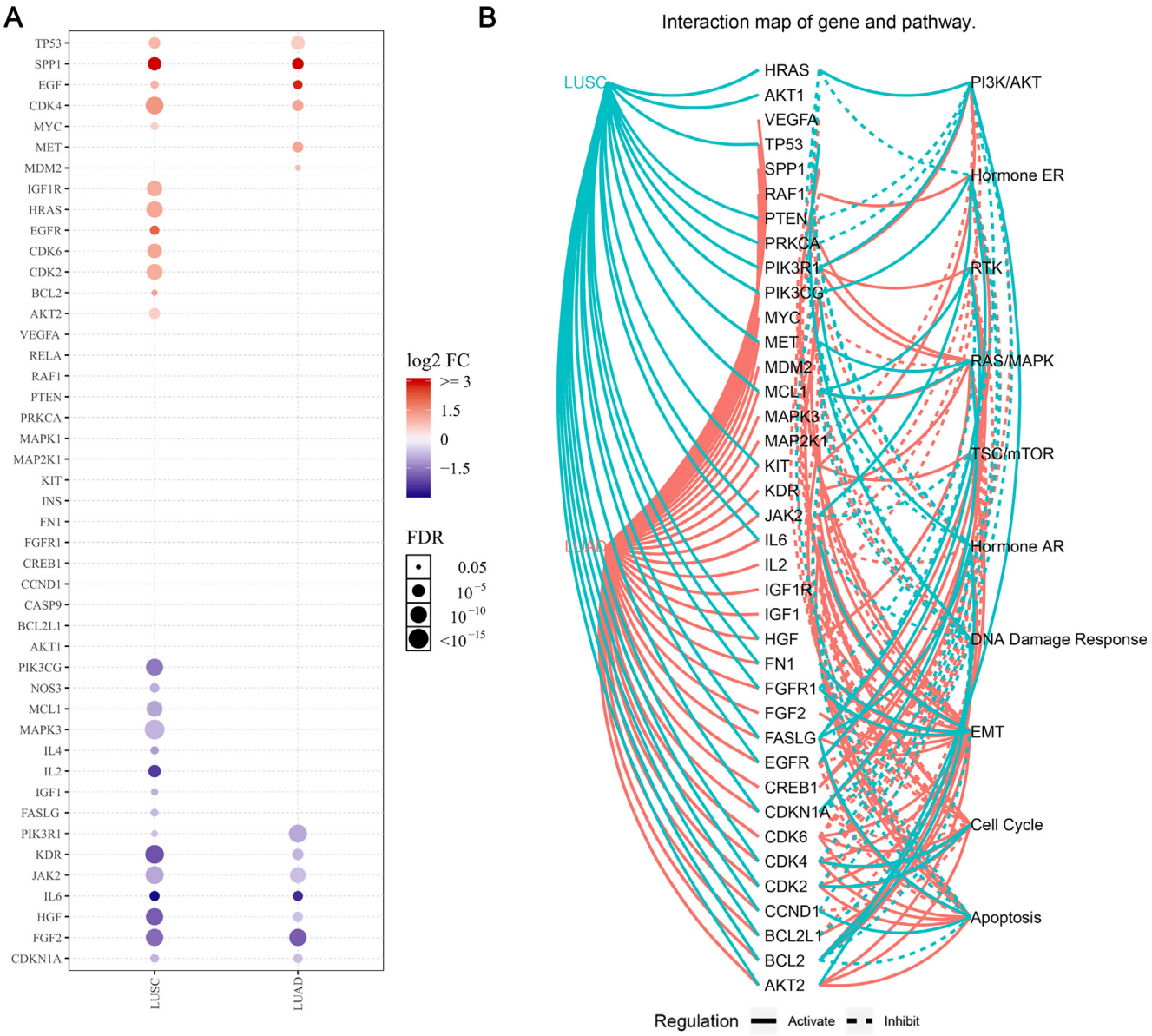

Fig. 5 The expression and pathways activity analysis of guava leaf constituent target genes in the PI3K-Akt signaling pathway. (A) The mRNA expression profile of genes. The dots represent the fold change; the blue color indicates downregulation while the red color indicates upregulation. The size of the dot is proportional to the expression foldchange (FC). (B) Pathway activity analysis.

DNA damage response, hormone AR, TSC/mTOR, RAS/MAPK, RTK and hormone ER pathways.

3.6. Molecular docking

The previous drug-disease interaction gene network topological analysis showed that the 10 genes with the strongest interaction were STAT3, TP53, AKT1, JUN, IL6, VEGFA, SRC, TNF, HRAS, and CDKN1A, which are effective in the "Guava leaf-constituent category" network. The Cytoscape interaction network of component-genes showed that the five compounds with strong interaction between guava leaf constituents and lung cancer genes were quercetin, genistein, apigenin, ursolic acid, and daidzein. The five compounds and 10 target proteins were molecularly docked by online molecular docking on the systemsDock website. The score of the database system docking was between 0 and 10. The larger the docking score, the better the docking effect, and the greater the binding activity between the docking molecule and the target. A docking score greater than 4.25 indicates that a ligand

Table 9 Docking results of receptor proteins and ligand compounds.

Ligand ID	compounds	Receptor proteins	PDB ID	gene	Docking results
5,280,343	quercetin	Signal transducer and activator of transcription 3	1BG1	STAT3	7.475
5,280,863	kaempferol	Signal transducer and activator of transcription 3	1BG1	STAT3	7.437
5,280,961	Genistein	Signal transducer and activator of transcription 3	1BG1	STAT3	7.809
5,281,708	Daidzein	Signal transducer and activator of transcription 3	1BG1	STAT3	7.811
64,945	ursolic acid	Signal transducer and activator of transcription 3	1BG1	STAT3	4.88
5,280,343	quercetin	Cellular tumor antigen p53	5MGT	TP53	6.658
5,280,863	kaempferol	Cellular tumor antigen p53	5MGT	TP53	6.689
5,280,961	Genistein	Cellular tumor antigen p53	5MGT	TP53	6.669
5,281,708	Daidzein	Cellular tumor antigen p53	5MGT	TP53	6.662
64,945	ursolic acid	Cellular tumor antigen p53	5MGT	TP53	5.464
5,280,343	quercetin	RAC-alpha serine/threonine-protein kinase	3CQW	AKT1	6.847
5,280,863	kaempferol	RAC-alpha serine/threonine-protein kinase	3CQW	AKT1	6.858
5,280,961	Genistein	RAC-alpha serine/threonine-protein kinase	3CQW	AKT1	6.824
5,281,708	Daidzein	RAC-alpha serine/threonine-protein kinase	3CQW	AKT1	6.85
64,945	ursolic acid	RAC-alpha serine/threonine-protein kinase	3CQW	AKT1	8.331
5,280,343	quercetin	Interleukin-6	1ALU	IL6	6.684
5,280,863	kaempferol	Interleukin-6	1ALU	IL6	6.656
5,280,961	Genistein	Interleukin-6	1ALU	IL6	6.632
5,281,708	Daidzein	Interleukin-6	1ALU	IL6	6.663
64,945	ursolic acid	Interleukin-6	1ALU	IL6	4.936
5,280,343	quercetin	Transcription factor AP-1	5TO1	JUN	6.569
5,280,863	kaempferol	Transcription factor AP-1	5TO1	JUN	6.548
5,280,961	Genistein	Transcription factor AP-1	5TO1	JUN	6.59
5,281,708	Daidzein	Transcription factor AP-1	5TO1	JUN	6.637
64,945	ursolic acid	Transcription factor AP-1	5TO1	JUN	4.892
5,280,343	quercetin	Vascular endothelial growth factor A	6BFT	VEGFA	5.849
5,280,863	kaempferol	Vascular endothelial growth factor A	6BFT	VEGFA	5.937
5,280,961	Genistein	Vascular endothelial growth factor A	6BFT	VEGFA	6.601
5,281,708	Daidzein	Vascular endothelial growth factor A	6BFT	VEGFA	6.65
64,945	ursolic acid	Vascular endothelial growth factor A	6BFT	VEGFA	5.799
5,280,343	quercetin	Proto-oncogene tyrosine-protein kinase Src	2BDJ	SRC	6.46
5,280,863	kaempferol	Proto-oncogene tyrosine-protein kinase Src	2BDJ	SRC	6.785
5,280,961	Genistein	Proto-oncogene tyrosine-protein kinase Src	2BDJ	SRC	6.246
5,281,708	Daidzein	Proto-oncogene tyrosine-protein kinase Src	2BDJ	SRC	6.789
64,945	ursolic acid	Proto-oncogene tyrosine-protein kinase Src	2BDJ	SRC	7.927
5,280,343	quercetin	Tumor necrosis factor	3ALQ	TNF	4.904
5,280,863	kaempferol	Tumor necrosis factor	3ALQ	TNF	5.01
5,280,961	Genistein	Tumor necrosis factor	3ALQ	TNF	5.109
5,281,708	Daidzein	Tumor necrosis factor	3ALQ	TNF	5.063
64,945	ursolic acid	Tumor necrosis factor	3ALQ	TNF	5.945
5,280,343	quercetin	GTPase HRas	6D5W	HRAS	6.434
5,280,863	kaempferol	GTPase HRas	6D5W	HRAS	6.582
5,280,961	Genistein	GTPase HRas	6D5W	HRAS	6.595
5,281,708	Daidzein	GTPase HRas	6D5W	HRAS	6.605
64,945	ursolic acid	GTPase HRas	6D5W	HRAS	7.867
5,280,343	quercetin	Cyclin-dependent kinase inhibitor 1	3TS8	CDKN1A	5.02
5,280,863	kaempferol	Cyclin-dependent kinase inhibitor 1	3TS8	CDKN1A	5.023
5,280,961	Genistein	Cyclin-dependent kinase inhibitor 1	3TS8	CDKN1A	4.663
5,281,708	Daidzein	Cyclin-dependent kinase inhibitor 1	3TS8	CDKN1A	4.94
64,945	ursolic acid	Cyclin-dependent kinase inhibitor 1	3TS8	CDKN1A	8.148

has a certain binding activity with a receptor; a score greater than 5.0 indicates a better binding activity; a score greater than 7.0 indicates a strong binding activity (Hsin et al., 2016). The PDB ID of the 10 genes was molecularly docked with the five compounds. The docking scores of all compounds and proteins were greater than 4.25, indicating the presence of binding activity. The molecular docking results are shown in Table 9.

A heat map of the molecular docking is shown in Fig. 6A. The deeper the color, the better the docking effect. The effect of molecular docking is also shown by the heat map. Table 9 and Fig. 6A showed that the compound with the highest binding activity to the protein receptor STAT3 was genistein; that with the highest binding activity to the protein receptor TP53 was kaempferol; that with the highest binding activity to the protein receptor AKT1 was kaempferol; that with the highest binding activity to the protein receptor AKT1 was quercetin; that with the highest binding activity to the protein receptor JUN was daidzein; that with the highest binding activity to the protein receptor VEGFA was genistein; that with the highest binding activity to the protein receptor SRC was ursolic acid; that with the highest binding activity to the protein receptor TNF was ursolic acid; that with the highest binding activity to the protein receptor HRAS was ursolic acid; and that with the highest binding activity to the protein receptor CDKN1A was ursolic Acid.

The 3D and 2D structures of their docking are shown in Table 10. In the 2D docking diagram of the third column, there is a specific case where the ligand binds to the receptor, and the surrounding red bar represents a bond-free protein residue within the ligand; the structure linked by the bat is a ligand compound and is subjected to the body protein. Purple represents a ligand compound; yellow represents a receptor protein. Red font represents the binding mode between the ligand and the receptor; the green dotted line represents a hydrogen bond. In these docking results, the docking activity of the receptor protein AKT1 and the ligand ursolic acid was 8.331, which was bound by Met 227 (A), Glu234 (A), and Thr291 (A); the receptor protein CDKN1A and the ligand compound ursolic acid, with docking activity of 8.148, and bound by a hydrogen bond with Asn247 (B) and Met246 (B), with bond lengths of 3.12 and 2.76, respectively, as well as with Cys242 (B), Met243 (A), Asn239 (B), Leu137 (B), Cys238 (B), Arg175 (B), and Arg174 (B), which directly bound.

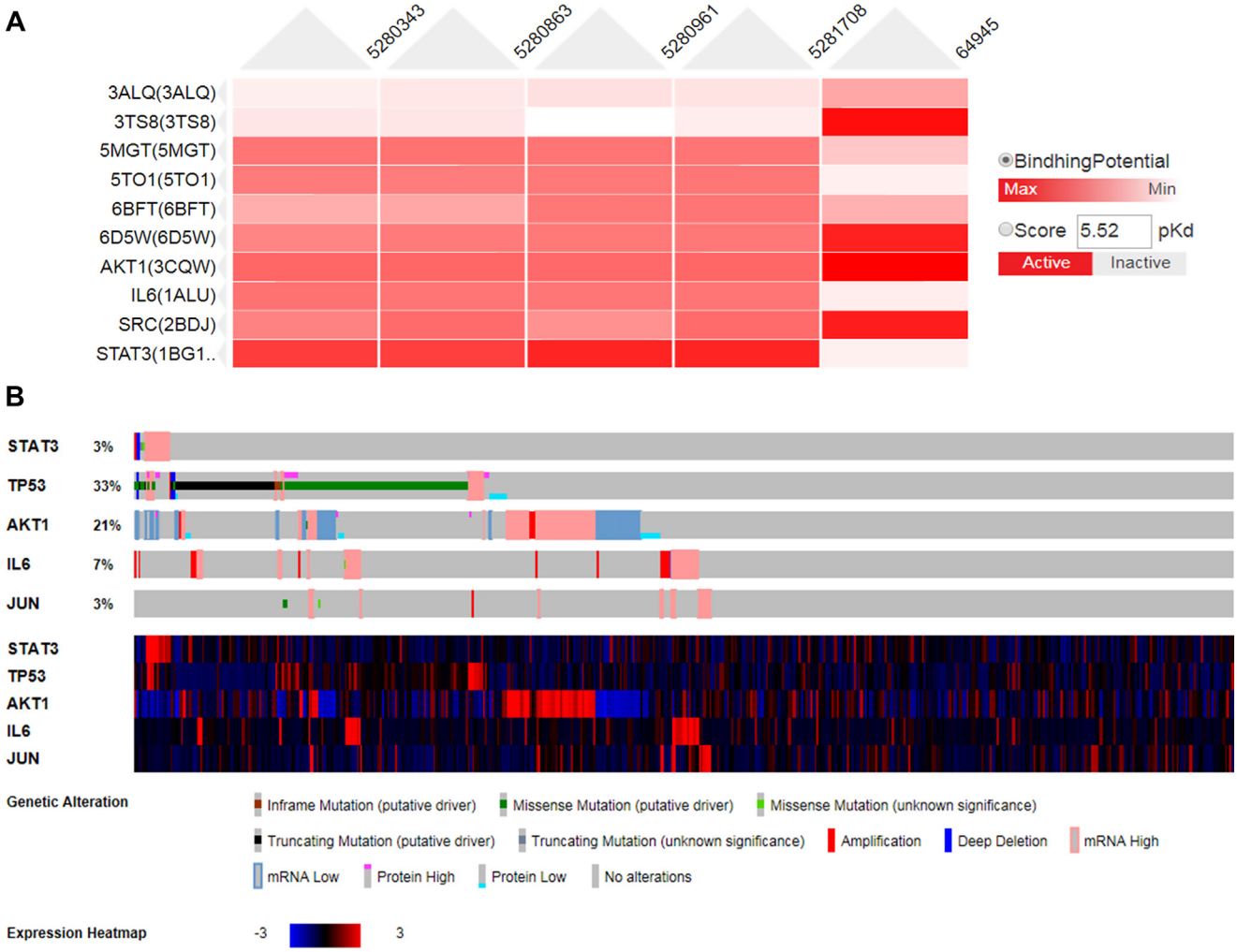

Fig. 6 Molecular docking. (A) A heat map showing the docking of receptor protein and ligand. (B) A diagram showing the genetic variation in lung squamous cell carcinoma.

Table 10 Molecular docking diagrams of the 3D and 2D structure.

Docking result of 3ALQ and ursolic acid	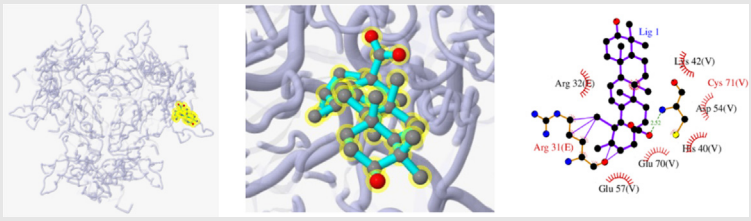
Docking result of 3TS8 and ursolic acid	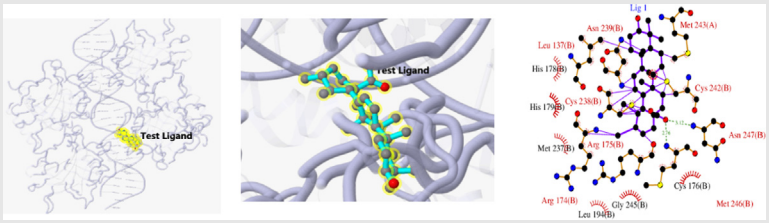
Docking result of 5GMT and kaempferol	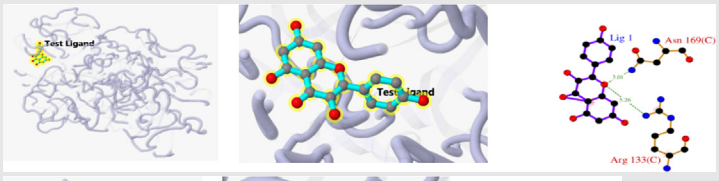
Docking result of 5TO1 and Daidzein	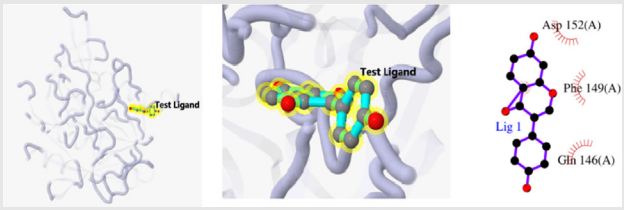
Docking result of 6BFT and Genistein	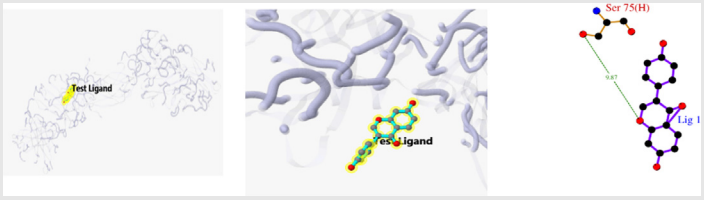
Docking result of 6D5W and ursolic acid	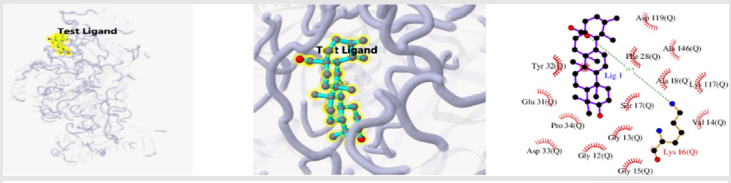
Docking result of 3CQW and kaempferol	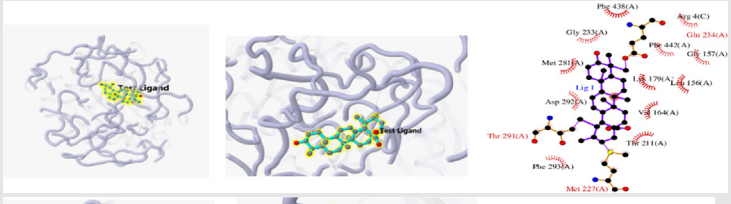
Docking result of 1ALU and quercetin	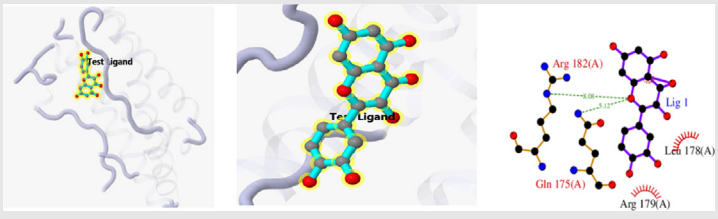

(*continued on next page*)

Table 10 (*continued*)

Docking result of 2BDJ and ursolic acid	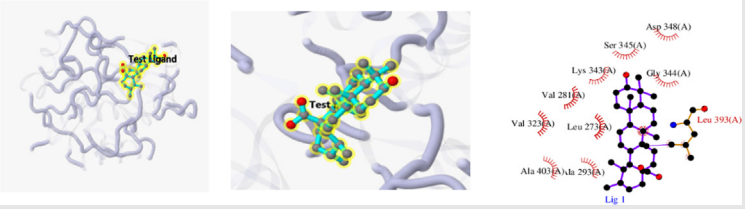
Docking result of 1BG1 and Daidzein	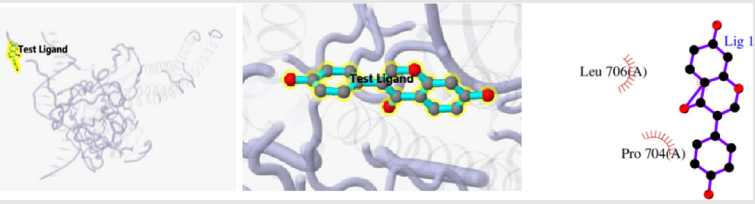

3.7. cBioPortal analysis

cBioPortal is a database used for tumor research. The expression of the genes STAT3, TP53, AKT1, IL6, and JUN in 501 patients with lung squamous cell carcinoma was studied. The expression of these genes in the selected lung cancer samples is shown in Fig. 6B. The first part is the expression of genes, including inframe mutation, missense mutation, truncating mutation, amplification, deep deletion, mRNA level upregulation (mRNA High), mRNA level downregulation (mRNA Low), and no alterations. The second part is a heat map of the gene mRNA levels.

According to the data in Fig. 6B, TP53 and AKT1 were highly expressed in these 501 cancer patients. TP53 was mainly expressed in patients with mutations (129 cases, 25.75%), increased copy number (1 case, 0.2%), mRNA level upregulation (6 cases, 1.2%), high protein level (5 cases, 1%), low protein level (8 cases, 1.8%), and multiple alterations (17 cases, 3.39%). AKT1 was expressed mainly in patients with mutations (1 case, 0.2%), increased copy number (5 cases, 1%), mRNA level upregulation (34 cases, 6.79%), mRNA level downregulation (34 cases, 6.79%), high protein level (2 cases, 0.4%), low protein level (15 cases, 2.99%), and multiple alterations (16 cases, 3.19%).

4. Discussion

Guava leaves are medicinal herbs with various pharmacological effects and a wide range of research and development significance. Guava leaves also have certain antitumor effects. Lung cancer is a common tumor. Currently, there is no particularly effective method for the diagnosis and treatment of lung cancer. Image detection is a commonly used diagnostic method (Hong et al., 2019), followed by genetic diagnosis (Munne and Wells, 2002). Lung cancer has a very low cure rate, and recent approaches to treat lung cancer include immunotherapy, radiotherapy, and targeted therapy (Alasti et al., 2006; Petrosyan et al., 2012; Tsang et al., 2014; Zhang et al., 2019). In this study, the role of guava leaves in lung cancer was studied by network pharmacology to elucidate their correlation and provide a relevant basis for experimental research. In recent years, the pharmacology of traditional Chinese medicine has been continuously developed and has occupied a place in medical research.

From the research point of view, examination of the potential intersection of guava leaf potential target and lung cancer genes revealed 153 common genes, and the interaction between STAT3, TP53, AKT1, IL6, JUN, and VEGFA was the strongest. Using the 66 compounds in guava leaves and the 153 genes, we constructed a "guava leaf-constituent category-active constituent-gene" network", and our results showed that the compounds quercetin, genistein, apigenin, ursolic acid, daidzein, and lung cancer showed the strongest effect. The proteins with the strongest interaction were VDR, CDK2, MAP2K1, CDK6, MET, ABL1, PPARG, IL2, EGFR, and PGR, indicating that these genes interacted with most constituents of guava leaves, showing that these constituents have high antitumor activities.

GO annotation is an important means to examine the function of gene products (Leale et al., 2018). Through GO analysis, in biological processes, enrichment information includes apoptosis, programmed cell death, cell proliferation, etc.; in terms of cellular components, enrichment Information includes platelets, cell membranes, protein kinases, etc.; in terms of molecular function, it is mainly reflected in enzyme activity and regulation of enzyme activity.

KEGG enrichment analysis provides information on integrated metabolic pathways including metabolism, membrane trafficking, signal processing, and cell cycle. The PI3K-Akt signaling pathway is a typical tumor signaling pathway. In many primary and metastatic human cancers, PTEN activity is lost owing to mutations, deletions, or high-frequency silencing of promoter methylation. It is important for prediction in targeted therapy (Fresno Vara et al., 2004; Carnero et al., 2008; Ma and Hu, 2013). EGFR tyrosine kinases are important for the treatment of non-small cell lung cancer, including monoclonal antibodies. The current clinical representatives are cetuximab and panitumumab as well as EGFR-tyrosine kinase inhibitor. The combination inhibits the binding site of ATP and tyrosine kinase, thereby cutting the downstream signaling pathway and exerting antitumor effect (Toulabi and Ryan, 2018). EGFR is of great significance in the study of non-small cell lung cancer and has potential implications for drug therapy (Mead et al., 1980; Marchetti et al., 2005). In the small

cell lung cancer pathway, the tumor suppressor genes are p53, PTEN, RB, and FHIT. ECM activates membrane receptors, and through ITGA and ITGB conduction, activates FAK conduction to activate PI3K activity and express the PKB/AKT signaling pathway. Through continuous phosphorylation and activation of IκBα, the free NF-κB signal is activated into the nucleus for gene network regulation. STAT3 and VEGF may play a reverse regulatory role on the metastasis of lung cancer (Wang et al., 2011). The p53 gene also has an antitumor effect, and Ad-p53 combined with chemotherapy can reverse the chemoresistance of tumor cells and produce a synergistic antitumor effect (Matsubara et al., 2001; Meng and El-Deiry, 2002). In addition, there are other genes expressed in lung cancer that were targeted by guava leaves, representing a potential research direction as clinical anticancer targets.

Analysis of lung squamous cell carcinoma by the cBioPortal tumor database revealed that the genes targeted by Chinese medicine and disease genes are highly expressed in cancer patients, and can undergo mutations, such as addition and deletion, and expression regulation. TP53 and AKT1 were the two most strongly expressed genes in the cancer patients surveyed. Hence, different compounds in guava leaves regulated the same target, and one compound regulated multiple targets and participated in multiple pathways and biological processes, reflecting the multi-target and multi-channel characteristics of guava leaves.

5. Conclusions

Through network pharmacology research, we found that guava leaves had potential targets that interacted with various tumors, regulating the signaling pathways of cancers. The PI3K-Akt signaling pathway, an important signaling pathway in the study of tumor processes, regulates the proliferation of tumor cells and plays a role in tumor cell migration, tumor adhesion, tumor angiogenesis, and extracellular matrix degradation (Chatterjee et al., 2013; Liu et al., 2014; Wang et al., 2016a). The TP53 gene is an important tumor suppressor gene involved in many gene network regulation processes, and has a reference significance in the research and development of new drugs and targeted therapy.

Many of the pharmacological effects of guava leaves are yet to be developed. There are many compounds in guava leaves. At present, antitumor studies on guava leaves are still lacking, although some studies have shown that guava leaves exert antitumor effects. This study preliminarily verified the pharmacological basis and the related mechanism of the antitumor effect of guava leaves, providing a foundation for further research. It is also hoped that specific experiments will be carried out to verify the pharmacological effects of guava leaves against tumors. If successful, the lack of cancer research on guava leaves will be overcame. In addition, network pharmacology is a hot topic of research; we hope to conduct more research projects in the future to provide a basis for future research on new drugs.

6. Data availability

The data used to support the findings of this study are included within the article.

Author contribution

LJ has made substantial contributions to conception and design, interpretation of data, and manuscript writing. WJ has made substantial contributions to acquisition and analysis of data. YQ and JL received the funding supporting for the study. YW has made substantial contributions to acquisition of data.

Funding

This work was supported by the Guangxi Natural Science Foundation Program [Grant number 2018GXNSFAA138140]; the Basic Competence Improvement Project for Middle and Young Teachers in Guangxi universities [Grant number KY2016LX281]; the Hechi University School Research Project [Grant number 2014QN-N005]; and the Hechi University - High-level Talent Research Startup Project [Grant number XJ2018GKQ014].

Declaration of Competing Interest

The authors declare that they have no known competing financial interests or personal relationships that could have appeared to influence the work reported in this paper.

References

Alasti, H., Cho, Y.B., Vandermeer, A.D., Abbas, A., Norrlinger, B., Shubbar, S., Bezjak, A., 2006. A novel four-dimensional radiotherapy method for lung cancer: imaging, treatment planning and delivery. Phys. Med. Biol. 51, 3251–3267. https://doi.org/10.1088/0031-9155/51/12/017.

Alnaqeeb, M., Mansor, K.A., Mallah, E.M., Ghanim, B.Y., Idkaidek, N., Qinna, N.A., 2019. Critical pharmacokinetic and pharmacodynamic drug-herb interactions in rats between warfarin and pomegranate peel or guava leaves extracts. BMC Complement. Altern. Med. 19, 29. https://doi.org/10.1186/s12906-019-2436-5.

Ashraf, A., Sarfraz, R.A., Rashid, M.A., Mahmood, A., Shahid, M., Noor, N., 2016. Chemical composition, antioxidant, antitumor, anticancer and cytotoxic effects of Psidium guajava leaf extracts. Pharm. Biol. 54, 1971–1981. https://doi.org/10.3109/13880209.2015.1137604.

Bauer-Mehren, A., Rautschka, M., Sanz, F., Furlong, L.I., 2010. DisGeNET: a Cytoscape plugin to visualize, integrate, search and analyze gene-disease networks. Bioinformatics 26, 2924–2926. https://doi.org/10.1093/bioinformatics/btq538.

Boezio, B., Audouze, K., Ducrot, P., Taboureau, O., 2017. Network-based approaches in pharmacology. Mol. Inform. 36. https://doi.org/10.1002/minf.201700048.

Carnero, A., Blanco-Aparicio, C., Renner, O., Link, W., Leal, J.F., 2008. The PTEN/PI3K/AKT signalling pathway in cancer, therapeutic implications. Curr. Cancer Drug Targets 8, 187–198. https://doi.org/10.2174/156800908784293659.

Chatterjee, M., Andrulis, M., Stuhmer, T., Muller, E., Hofmann, C., Steinbrunn, T., 2013. The PI3K/Akt signaling pathway regulates the expression of Hsp70, which critically contributes to Hsp90-chaperone function and tumor cell survival in multiple myeloma. Haematologica 98, 1132–1141. https://doi.org/10.3324/haematol.2012.066175.

Chen, W.Q., Zuo, T.T., Zheng, R.S., Zeng, H.M., Zhang, S.W., He, J., 2017. Lung cancer incidence and mortality in China in 2013. Zhonghua Zhong Liu Za Zhi 39, 795–800. https://doi.org/10.3760/cma.j.issn.0253-3766.2017.10.015.

Danhof, M., 2016. Systems pharmacology – towards the modeling of network interactions. Eur. J. Pharm. Sci. 94, 4–14. https://doi.org/10.1016/j.ejps.2016.04.027.

Ebrahimi, S., Hosseini, M., Shahidsales, S., Maftouh, M., Ferns, G.A., Ghayour-Mobarhan, M., Mahdi Hassanian, S., Avan, A., 2017. Targeting the Akt/PI3K signaling pathway as a potential therapeutic strategy for the treatment of pancreatic cancer. Curr. Med. Chem. 24, 1321–1331. https://doi.org/10.2174/0929867324666170206142658.

Feng, X.H., Wang, Z.H., Meng, D.L., Li, X., 2015. Cytotoxic and antioxidant constituents from the leaves of Psidium guajava. Bioorg. Med. Chem. Lett. 25, 2193–2198. https://doi.org/10.1016/j.bmcl.2015.03.058.

Fresno Vara, J.A., Casado, E., de Castro, J., Cejas, P., Belda-Iniesta, C., Gonzalez-Baron, M., 2004. PI3K/Akt signalling pathway and cancer. Cancer Treat. Rev. 30, 193–204. https://doi.org/10.1016/j.ctrv.2003.07.007.

Gutierrez, R.M., Mitchell, S., Solis, R.V., 2008. Psidium guajava: a review of its traditional uses, phytochemistry and pharmacology. J. Ethnopharmacol. 117, 1–27. https://doi.org/10.1016/j.jep.2008.01.025.

Hong, G.S., Do, K.H., Lee, C.W., 2019. Added value of bone suppression image in the detection of subtle lung lesions on chest radiographs with regard to reader's expertise. J. Korean Med. Sci. 34,. https://doi.org/10.3346/jkms.2019.34.e250 e250.

Hsin, K.Y., Ghosh, S., Kitano, H., 2013. Combining machine learning systems and multiple docking simulation packages to improve docking prediction reliability for network pharmacology. PLoS ONE 8,. https://doi.org/10.1371/journal.pone.0083922 e83922.

Hsin, K.Y., Matsuoka, Y., Asai, Y., Kamiyoshi, K., Watanabe, T., Kawaoka, Y., Kitano, H., 2016. systemsDock: a web server for network pharmacology-based prediction and analysis. Nucleic Acids Res. 44, W507–513. https://doi.org/10.1093/nar/gkw335.

Hu, Q.N., Deng, Z., Tu, W., Yang, X., Meng, Z.B., Deng, Z.X., Liu, J., 2014. VNP: interactive visual network pharmacology of diseases, targets, and drugs. CPT Pharmacometrics Syst. Pharmacol. 3,. https://doi.org/10.1038/psp.2014.1 e105.

Kandaswami, C., Lee, L.T., Lee, P.P., Hwang, J.J., Ke, F.C., Huang, Y.T., Lee, M.T., 2005. The antitumor activities of flavonoids. Vivo 19, 895–909.

Kim, S., Thiessen, P.A., Bolton, E.E., Chen, J., Fu, G., Gindulyte, A., Han, L., He, J., He, S., Shoemaker, B.A., Wang, J., Yu, B., Zhang, J., Bryant, S.H., 2016. PubChem substance and compound databases. Nucleic Acids Res. 44, D1202–D1213. https://doi.org/10.1093/nar/gkv951.

Kohl, M., Wiese, S., Warscheid, B., 2011. Cytoscape: software for visualization and analysis of biological networks. Methods Mol. Biol. 696, 291–303. https://doi.org/10.1007/978-1-60761-987-1_18.

Leale, G., Baya, A.E., Milone, D.H., Granitto, P.M., Stegmayer, G., 2018. Inferring unknown biological function by integration of GO annotations and gene expression data. IEEE/ACM Trans. Comput. Biol. Bioinform. 15, 168–180. https://doi.org/10.1109/tcbb.2016.2615960.

Lee, S.B., Park, H.R., 2010. Anticancer activity of guava (Psidium guajava L.) branch extracts against HT-29 human colon cancer cells. J. Med. Plants Res. 4, 891–896.

Lee, S., 2015. Systems biology – a pivotal research methodology for understanding the mechanisms of traditional medicine. J. Pharmacopuncture 18, 11–18. https://doi.org/10.3831/KPI.2015.18.020.

Liu, J., Zhang, C., Lin, M., Zhu, W., Liang, Y., Hong, X., Zhao, Y., Young, K.H., Hu, W., Feng, Z., 2014. Glutaminase 2 negatively regulates the PI3K/AKT signaling and shows tumor suppression activity in human hepatocellular carcinoma. Oncotarget 5, 2635–2647. https://doi.org/10.18632/oncotarget.1862.

Liu, X., Ouyang, S., Yu, B., Liu, Y., Huang, K., Gong, J., Zheng, S., Li, Z., Li, H., Jiang, H., 2010. PharmMapper server: a web server for potential drug target identification using pharmacophore mapping approach. Nucleic Acids Res. 38, W609–614. https://doi.org/10.1093/nar/gkq300.

Lu, Q., He, L., Li, D., Wang, K., 2016. Terpenoids progress in the anti-tum or research. Heilongjiang Sci. Technol. Inform. 30, 149–151.

Luo, Y., Peng, B., Wei, W., Tian, X., Wu, Z., 2019. Antioxidant and anti-diabetic activities of polysaccharides from guava leaves. Molecules 24. https://doi.org/10.3390/molecules24071343.

Ma, X., Hu, Y., 2013. Targeting PI3K/Akt/mTOR cascade: the medicinal potential, updated research highlights and challenges ahead. Curr. Med. Chem. 20 (24), 2991–3010. https://doi.org/10.2174/09298673113209990124.

Marchetti, A., Martella, C., Felicioni, L., Barassi, F., Salvatore, S., Chella, A., 2005. EGFR mutations in non-small-cell lung cancer: analysis of a large series of cases and development of a rapid and sensitive method for diagnostic screening with potential implications on pharmacologic treatment. J. Clin. Oncol. 23, 857–865. https://doi.org/10.1200/jco.2005.08.043.

Matsubara, H., Maeda, T., Gunji, Y., Koide, Y., Asano, T., Ochiai, T., 2001. Combinatory anti-tumor effects of electroporation-mediated chemotherapy and wild-type p53 gene transfer to human esophageal cancer cells. Int. J. Oncol. 18, 825–829. https://doi.org/10.3892/ijo.18.4.825.

Mead, G.M., Arnold, A.M., Green, J.A., Williams, C.J., Whitehouse, J.M., 1980. Small-cell lung cancer. Lancet 1, 252. https://doi.org/10.1016/s0140-6736(80)90733-3.

Meng, R.D., El-Deiry, W.S., 2002. "CHAPTER 18 - Cancer Gene Therapy with the p53 Tumor Suppressor Gene," in Gene Therapy of Cancer (Second Edition), eds. E.C. Lattime & S.L. Gerson. (San Diego: Academic Press), 299-313.

Munne, S., Wells, D., 2002. Preimplantation genetic diagnosis. Curr. Opin. Obstet. Gynecol. 14, 239–244. https://doi.org/10.1097/00001703-200206000-00001.

Ouyang, W., Zhu, X.A., Liu, X.J., Yie, S.M., Zhao, L., Su, L., 2015. Spectroscopic characteristics of novel Psidium meroterpenoids isolated from guava leaves. Zhongguo Zhong Yao Za Zhi 40, 2898–2902.

Petrosyan, F., Daw, H., Haddad, A., Spiro, T., 2012. Targeted therapy for lung cancer. Anticancer Drugs 23, 1016–1021. https://doi.org/10.1097/CAD.0b013e3283585149.

Rafiemanesh, H., Mehtarpour, M., Khani, F., Hesami, S.M., Shamlou, R., Towhidi, F., Salehiniya, H., Makhsosi, B.R., Moini, A., 2016. Epidemiology, incidence and mortality of lung cancer and their relationship with the development index in the world. J. Thorac. Dis. 8, 1094–1102. https://doi.org/10.21037/jtd.2016.03.91.

Ru, J., Li, P., Wang, J., Zhou, W., Li, B., Huang, C., Li, P., Guo, Z., Tao, W., Yang, Y., Xu, X., Li, Y., Wang, Y., Yang, L., 2014. TCMSP: a database of systems pharmacology for drug discovery from herbal medicines. J. Cheminform. 6, 13. https://doi.org/10.1186/1758-2946-6-13.

Seo, J., Lee, S., Elam, M.L., Johnson, S.A., Kang, J., Arjmandi, B.H., 2014. Study to find the best extraction solvent for use with guava leaves (Psidium guajava L.) for high antioxidant efficacy. Food Sci. Nutr. 2, 174–180. https://doi.org/10.1002/fsn3.91.

Shao, M., Wang, Y., Huang, X.J., Fan, C.L., Zhang, Q.W., Zhang, X.Q., Ye, W.C., 2012a. Four new triterpenoids from the leaves of Psidium guajava. J. Asian Nat. Prod. Res. 14, 348–354. https://doi.org/10.1080/10286020.2011.653964.

Shao, M., Wang, Y., Jian, Y.Q., Huang, X.J., Zhang, D.M., Tang, Q.F., Jiang, R.W., Sun, X.G., Lv, Z.P., Zhang, X.Q., Ye, W.C., 2012b. Guadial A and psiguadials C and D, three unusual meroterpenoids from Psidium guajava. Org. Lett. 14, 5262–5265. https://doi.org/10.1021/ol302423b.

Song, C., Zhu, M., 2011. Research advancement of the antitumor effect and mechanisms of triterpenoid comprised by traditional Chinese medicine. J. Modern Oncol. 19, 1880–1883. https://doi.org/10.3969/j.issn.1672-4992.2210.09.66.

Toulabi, L., Ryan, B.M., 2018. Stressing the need to overcome EGFR tyrosine kinase inhibitor resistance. Transl. Lung Cancer Res. 7, S123–s126. https://doi.org/10.21037/tlcr.2018.03.05.

Tsang, M.W., Kam, M.K., Leung, S.F., Chan, A.T., 2014. Non-surgical treatment of lung cancer: personalised stereotactic ablative radiotherapy. Hong Kong Med. J. 20, 529–536. https://doi.org/10.12809/hkmj144269.

Wang, L., Liu, J., Zhong, Z., Gong, X., Liu, W., Shi, L., Li, X., 2016a. PTP4A3 is a target for inhibition of cell proliferatin, migration and invasion through Akt/mTOR signaling pathway in glioblastoma under the regulation of miR-137. Brain Res. 1646, 441–450. https://doi.org/10.1016/j.brainres.2016.06.026.

Wang, L., Tian, X., Wei, W., Chen, G., Wu, Z., 2016b. Fingerprint analysis and quality consistency evaluation of flavonoid compounds for fermented Guava leaf by combining high-performance liquid chromatography time-of-flight electrospray ionization mass spectrometry and chemometric methods. J. Sep. Sci. 39, 3906–3916. https://doi.org/10.1002/jssc.201600552.

Wang, M., Chen, G.Y., Song, H.T., Hong, X., Yang, Z.Y., Sui, G.J., 2011. Significance of CXCR4, phosphorylated STAT3 and VEGF-A expression in resected non-small cell lung cancer. Exp. Ther Med. 2, 517–522. https://doi.org/10.3892/etm.2011.235.

Wang, Y.L., Cui, T., Li, Y.Z., Liao, M.L., Zhang, H.B., Hou, W.B., 2019. Prediction of quality markers of traditional Chinese medicines based on network pharmacology. Chinese Herbal Med. https://doi.org/10.1016/j.chmed.2019.08.003.

Wu, P., Heins, Z.J., Muller, J.T., Katsnelson, L., de Bruijn, I., Abeshouse, A.A., 2019. Integration and analysis of CPTAC proteomics data in the context of cancer genomics in the cBioPortal. Mol. Cell. Proteomics 18, 1893–1898. https://doi.org/10.1074/mcp.TIR119.001673.

Wu, X.M., Wu, C.F., 2015. Network pharmacology: a new approach to unveiling Traditional Chinese Medicine. Chin. J. Nat. Med. 13, 1–2. https://doi.org/10.1016/s1875-5364(15)60001-2.

Xing, D.F., Xu, C.D., Liao, X.Y., Xing, T.Y., Cheng, S.P., Hu, M.G., 2019. Spatial association between outdoor air pollution and lung cancer incidence in China. BMC Public Health 19, 1377. https://doi.org/10.1186/s12889-019-7740-y.

Zhang, R., Zhu, Z., Lv, H., Li, F., Sun, S., Li, J., 2019. Immune checkpoint blockade mediated by a small-molecule nanoinhibitor targeting the PD-1/PD-L1 pathway synergizes with photodynamic therapy to elicit antitumor immunity and antimetastatic effects on breast cancer. Small e1903881. https://doi.org/10.1002/smll.201903881.